



Mechanics of the *Toxoplasma gondii* oocyst wall

Aurélien Dumètre, Jitender P Dubey, David J P Ferguson, Pierre Bongrand,
Nadine Azas, Pierre-Henri Puech

► To cite this version:

Aurélien Dumètre, Jitender P Dubey, David J P Ferguson, Pierre Bongrand, Nadine Azas, et al..
Mechanics of the *Toxoplasma gondii* oocyst wall. *Proceedings of the National Academy of Sciences of the United States of America*, 2013, 110, pp.11535 - 11540. 10.1073/pnas.1308425110 . hal-01104911

HAL Id: hal-01104911

<https://hal.science/hal-01104911>

Submitted on 19 Jan 2015

HAL is a multi-disciplinary open access archive for the deposit and dissemination of scientific research documents, whether they are published or not. The documents may come from teaching and research institutions in France or abroad, or from public or private research centers.

L'archive ouverte pluridisciplinaire **HAL**, est destinée au dépôt et à la diffusion de documents scientifiques de niveau recherche, publiés ou non, émanant des établissements d'enseignement et de recherche français ou étrangers, des laboratoires publics ou privés.



Distributed under a Creative Commons Attribution - NonCommercial - NoDerivatives| 4.0
International License

1 Author edited

2

3 **Mechanics of the *Toxoplasma gondii* oocyst wall**

4

5 Aurélien Dumètre^{a,1}, Jitender P. Dubey^{b,1}, David J. P. Ferguson^c, Pierre Bongrand^{d,e},

6 Nadine Azas^a, Pierre-Henri Puech^{d,1}

7

8^a UMR MD3 Infections Parasitaires, Transmission, Physiopathologie et Thérapeutique,

9 Aix-Marseille Université, Faculté de Pharmacie, 27 Bd Jean Moulin, 13385 Marseille

10 Cedex 05, France

11^b United States Department of Agriculture, Agricultural Research Service, Beltsville

12 Agricultural research Center, Animal Parasitic Diseases Laboratory, Building 1001,

13 Beltsville, MD 20705-2350, USA

14^c Nuffield Department of Clinical Laboratory Science, University of Oxford, John

15 Radcliffe Hospital, Oxford, United Kingdom

16^d INSERM UMR 1067 / CNRS UMR 7333, Adhésion Cellulaire et Inflammation, Aix-

17 Marseille Université, Bat. TRP2 Bloc 5 Entrée B 3eme étage, Case 937, 163 Av de

18 Luminy, 13288 Marseille Cedex 09, France

19^e Laboratoire d'Immunologie, Hôpital de la Conception, 147 Bd Baille, 13385 Marseille,

20 France

21 Contributed by Jitender P. Dubey, ---(sent for review October 1, 2012)

22¹ Send correspondence to jitender.dubey@ars.usda.gov, aurelien.dumetre@univ-amu.fr

23 or pierre-henri.puech@inserm.fr

24Abstract

25The ability of microorganisms to survive under extreme conditions is closely related to
26the physicochemical properties of their wall. In the ubiquitous protozoan parasite
27*Toxoplasma gondii*, the oocyst stage possesses a bilayered wall that protects the dormant
28but potentially infective parasites from harsh environmental conditions until their
29ingestion by the host. None of the common disinfectants are effective in killing the
30parasite, since the oocyst wall acts as a primary barrier to physical and chemical attacks.
31Here, we address the structure and chemistry of the wall of the *T. gondii* oocyst by
32combining wall surface treatments, fluorescence imaging, electron microscopy and
33measurements of its mechanical characteristics by using Atomic Force Microscopy
34(AFM). Elasticity and indentation measurements indicated that the oocyst wall resembles
35common plastic materials, based on the Young moduli, E , evaluated by AFM. Our study
36demonstrates that the inner layer is as robust as the bilayered wall itself. Besides wall
37mechanics, our results suggest important differences regarding the non specific adhesive
38properties of each layer. All together, these findings suggest a key biological role for the
39oocyst wall mechanics in maintaining the integrity of the *T. gondii* oocysts in the
40environment or after exposure to disinfectants, and therefore their potential infectivity to
41humans and animals.

42

43

44Introduction

45Resistance to physical and chemical degradation is essential for the perpetuation of the
46life cycle of environmentally exposed microbial pathogens. In the coccidian parasite
47*Toxoplasma gondii*, this function is served by the oocyst, the only stage of the parasite
48structurally equipped to survive in harsh environments (1). Oocyst-related infections in
49humans and other warm-blooded animals worldwide have been increasingly reported as
50more prevalent and severe than previously thought (2–6). Infections lead to possible
51deleterious ocular and neurological complications, and even death (7). In this context, a
52global effort has emerged to decipher the basic structures (8, 9) and biological processes
53of the oocyst (10–13) that allow the parasite to survive different environmental conditions
54and disinfectants (14–18).

55The oocyst is the result of sexual multiplication of *T. gondii* in the intestinal epithelium of
56cats (19–21). A few days post-infection, unsporulated (uninfective) spheroid oocysts (10
57x 12 μ m) are excreted in cat feces and become rapidly infective following aerobic
58sporulation (22). Sporulation results in different subpopulations of maturing oocysts
59during the first few days (22): unsporulated (NS), ‘sporoblast-staged’ (SB) and fully
60sporulated (SP) oocysts (11, 22). SP oocysts are ovoid, measure 11 x 13 μ m in size and
61have two sporocysts (6 x 8 μ m), each containing four infective banana-shaped
62sporozoites (2 x 6-8 μ m) (*SI Appendix*, Fig. S1) (23, 24).

63*Toxoplasma gondii* oocysts are highly resistant to environmental influences and this
64resistance to various physical and chemical stressors, including disinfectants such as UV,
65ozone, and chlorine-based products, is attributed to the oocyst wall (4, 25, 26). In
66contrast, oocysts are rapidly inactivated following exposure to temperatures above 60°C

67for few minutes (27). The oocyst wall is bilayered with the outer layer being thinner than
68the inner layer (24). The layers are not tightly bound to each other since the outer layer
69can be stripped off easily using sodium hypochlorite (10, 12, 22, and the present study).
70The oocyst wall is made of more than 90% proteins with several structural cysteine- and
71tyrosine-rich proteins having been identified in the outer layer only (13) or in whole
72oocyst wall fractions (10, 12). How these different proteins are processed and/or packed
73to form the oocyst wall is still not clear (8). Current models support a strong contribution
74of protein-tyrosine cross-linking in the formation and hardening of the oocyst wall in
75*Toxoplasma*-related coccidia (8, 12, 26, 28) and results in the development of its typical
76blue autofluorescence (AF) under UV excitation (10, 26, 28, 29) (*SI Appendix*, Fig. S1B).
77This complex polymeric organization also suggests an important robustness of the *T.*
78*gondii* oocyst wall in terms of mechanics (8, 26). Thus, measuring mechanical properties
79of the *T. gondii* oocyst wall appears to be relevant to addressing the respective roles of
80structure and chemistry of each layer of the oocyst wall in the overall resistance of the
81oocyst to various physical and chemical agents (8).

82Atomic Force Microscopy (AFM) is a rather new technique in biology that fits perfectly
83for this purpose (30). The AFM provides valuable information regarding the surface
84topography and/or allows force measurements in physiological media, with fixed or
85unfixed samples, from proteins to cells (31–33). AFM uses a finger-like tip, at the
86extremity of a very soft cantilever (30). This tip can be used to: (i) delineate the surface
87(imaging mode, (34–36)), (ii) indent the objects surface by pressing on them allowing
88measurement of their mechanical properties (force mode, mechanics, (37–40)) or (iii)
89probe the adhesion of surface molecules when decorated with suitable haptens and

90pulling the lever off the surface until all built bridges are broken. This allows direct
91quantifying of the force that these bridges can sustain (force mode, adhesion). For modes
92(ii) and (iii), the AFM cantilever is held at a given x,y above the sample (a surface or a
93cell) and ramped in z-direction. Measuring cantilever deflection as a function of piezo
94position produces force-extension curves (FC) (30).

95Using the AFM tip as a microindenter and using the part of the FC where the tip is
96pressed on the surface, one can gain information regarding the local elastic properties as
97measured as a Young's modulus, E , using a Hertz model for elastic indentation. E moduli
98measured for different eukaryotic cell types vary greatly from cell type to cell type and
99usually ranges from 1 kPa to several 100 kPa (37, 38). Using the part of the FC where the
100tip is retracted from the surface, adhesion force measurements can be performed and have
101been employed in cell biology, from single molecules measurements to cell/cell
102measurements (31, 41–47). The sensitivity of force determination is usually limited by
103the thermal noise of the system and the properties of the chosen cantilever (30).

104Here, we investigate using AFM the mechanics of the wall of *T. gondii* oocysts submitted
105to physical (heat inactivation) and chemical (bleach exposure) treatments separate or in
106combination in order to evaluate the contribution of each layer in the overall mechanics
107of the oocyst wall. Our results present a simple way to gently but firmly immobilize
108oocysts on surfaces to image them using fluorescence microscopy or test their mechanics
109using AFM under moderate forces. Our findings may be correlated to structural
110modifications of the oocyst wall and suggest a key biological role of the wall mechanics
111in maintaining the integrity of the *T. gondii* oocysts in the environment or exposed to
112disinfectants, therefore affecting potential infectivity to humans and animals.

113

114**Results**

115**Microscopic Characteristics of *T. gondii* Oocysts Following Sporulation in Water.** In
116order to evaluate the basic mechanics of the *T. gondii* oocyst wall, we limited the use of
117chemicals to avoid any modification of the wall structure due to handling or storage
118conditions. For this, oocysts were sporulated in water rather than in 2% aqueous sulfuric
119acid solution which is commonly used for oocyst sporulation and subsequent storage (11,
12022, 48). After a 5-day sporulation process, the oocyst suspension contained 18.6 ± 2.7 %
121of NS, 18.3 ± 6.4 % of SB and 63.0 ± 5.9 % of SP oocysts (*SI Appendix*, Fig. S1). All
122these different oocyst subpopulations exhibited the same typical autofluorescence (AF)
123under UV excitation (*SI Appendix*, Fig. S1B). Careful observation, before and during
124AFM experiments, was a key step to the exact categorization of the objects.

125

126**Characterization of the Bleach Effects on *T. gondii* Walls by Electron Microscopy.**
127Electron microscopy confirmed that control (H₂O-conserved) oocysts retained their
128typical double-layered wall (observed thickness ~50 nm, Fig. 1A,B). In contrast, the
129outer layer (observed thickness ~18-20 nm) was absent in bleach-treated oocysts with
130only the inner layer (observed thickness ~30 nm) remaining with, in certain cases, slight
131remnants of the outer layer persisting (Fig. 1C). The oocyst wall thicknesses that were
132observed here are consistent with but in the lower end of the reported values of such
133structures reported in literature (up to 100 nm for the bilayered wall) (24). It is interesting
134to note that the bilayered structure of the *T. gondii* sporocyst wall was maintained
135following bleach treatment of the oocyst wall (Fig. 1D,E).

137Characterization of *T. gondii* Walls by Fluorescence Microscopy. The properties of
138the wall of NS, SB and SP oocysts were first assessed microscopically by analyzing their
139reactivity to the monoclonal antibody (mAb) 4B6, which is specific to the inner layer of
140the oocyst wall (49). In order to induce structural modifications of the bilayered oocyst
141wall, the parasites were treated by bleach to remove the outer layer and/or heated at 80°C.
142In contrast to bleach treatment, heating oocysts at 80°C efficiently kills the sporozoites,
143however, the effects on the wall structure remain largely unknown. Oocysts exposed only
144to water during their maturation and storage served as controls. The percentages of
145oocysts at different maturing stages exposing partially or totally their inner wall
146following these different surface treatments are shown in Fig. 2. Corresponding immuno-
147fluorescence and AF representative images are shown in *SI Appendix*, Fig. S2.

148Between 21.2 and 25.6% of H₂O-exposed oocysts were labeled with antibody mAb 4B6
149(Fig. 2). A mixture of unstained to totally mAb 4B6-stained oocysts were observed
150irrespective of the oocyst developmental stage (*SI Appendix*, Fig. S2A). Fluorescent
151staining appeared randomly distributed at the oocyst surface, and ranged from almost
152continuous staining of the entire surface (*SI Appendix*, Fig. S2A, case 1) to very discrete
153patches (*SI Appendix*, Fig. S2A, case 2). In these conditions, 4B6 staining of the inner
154wall layer appeared to result from the infiltration of the antibody through cracks in the
155oocyst wall rather than the exposure of the outer aspect of the inner layer of the oocyst
156wall. This hypothesis was further supported by the fact that ~25-30% of H₂O-exposed
157oocysts were permeable to FITC in solution, again indicating possible openings in the

158oocyst wall (*SI Appendix*, Fig. S3). Irrespective of their 4B6 pattern, SB and SP oocysts
159were more autofluorescent than NS oocysts (*SI Appendix*, Fig. S2A and Fig. S4).

160Heating oocysts at 80°C for 10 min led to a significant reduction of the percentage of
1614B6-positive oocysts at all maturation stages (0.6-3.1%) (Fig. 2). The few positive
162oocysts observed were very faintly stained in localized areas of the oocyst wall (*SI*
163*Appendix*, Fig. S2B). In these experimental conditions, heating did not appear to alter
164significantly the microscopic structure or internal content of NS, SB and SP oocysts or
165the AF of the oocyst wall (*SI Appendix*, Fig. S2B compared to Fig. S2A).

166In contrast, there was a significant increase in mAb 4B6 staining of oocysts bleached
167with 3% bleach solution for 30 min (final mAb 4B6-labelled oocysts from 48.3 to 80.7%
168depending on the maturing stage) compared to control or heated oocysts (Fig. 2). In these
169experimental conditions, the antibody stained, at least partially, the inner layer of NS, SB
170and SP oocyst wall usually with a strong intensity (*SI Appendix*, Fig. S2C) indicating that
171modifications of the wall structure increase the access of mAb 4B6 to the outer aspect of
172the inner layer of the wall, but not its infiltration through it since only ~25-30% of
173bleach-exposed oocysts were again permeable to FITC due to possible fractures in their
174wall (*SI Appendix*, Fig. S3). We also observed that several bleach-treated oocysts
175displayed a reduced AF pattern of the oocyst wall compared to the control oocysts (*SI*
176*Appendix*, Fig. S4, suggesting possible differences in the biochemical content of the
177oocyst wall between untreated and bleach-treated oocysts.

178When bleached oocysts were subsequently heated at 80°C, the percentages of mAb 4B6-
179positive parasites were similar to that observed with bleaching alone (40.1-74.3%) (Fig.
1802). Microscopically, these oocysts had similar 4B6 and AF patterns compared to

181bleached-only oocysts, irrespective of the stage of maturation (*SI Appendix*, Fig. S2D
182compared to Fig. S2C). However, a few mAb 4B6-positive oocysts still had a very
183discrete wall AF (*SI Appendix*, Fig. S2D, case 5).

184

185**Attachment of the Oocysts for AFM Experiments.** The mechanical properties of the
186wall of H₂O-stored, bleach- and/or heat-treated oocysts at different maturing stages were
187then evaluated using AFM. For this, oocysts were first allowed to adhere onto Poly-L-
188Lysine (PLL)-coated glass microscopic slides prior to being approached by the AFM tip
189(*SI Appendix*, Fig. S5A,B,C). We verified that the coating procedure on glass did not
190change significantly the initial observed proportions of the different subpopulations of the
191oocysts irrespective of their pretreatment (*SI Appendix*, Fig. S5B). This coating procedure
192was suitable for firmly attaching the oocysts onto the glass surface thus allowing repeated
193contacts between the AFM tip and each oocyst at a preset contact force of 1 nN. The fine
194positioning of the AFM tip on top of the substructures (i.e. sporocysts) does not largely
195affect the measurements (*SI Appendix*, Fig. S5D,E).

196

197**Elastic Properties of the Oocyst Wall.** Following our immobilization protocol, repeated
198force curves were obtained for each adhered object (Fig. 3A,B). We observed that the
199indentation depth was <50 nm and typically ~ 20 nm (Fig. 3C,D) irrespective of the
200maturing oocyst stages or their pretreatment (*SI Appendix*, Table S1). This median
201indentation is of the same order of magnitude as the most outer layer of the oocyst wall
202(20 nm) and smaller than the thickness of the most inner layer (30 nm) as measured in
203EM micrographs. Following this, (i) in absence of bleach treatment, we concluded that

204we measured the mechanics of, if not the outer layer alone, the bilayered structure of the
205wall, and (ii) following bleach treatment, we were able to access the mechanical
206properties solely of the inner layer of the wall.

207Young moduli, E , obtained for NS, SB and SP H₂O-stored oocysts were typically in the
20810⁶-10⁷ Pa range and were not significantly different from each other (Fig. 3E,F). Those
209elevated E values are similar to the ones reported for artificial polymeric capsules of
210comparable thicknesses (50). The median E moduli showed no significant variation
211between the different maturing oocyst stages irrespective of the oocyst pretreatment (*SI*
212*Appendix*, Tables S2 and S4). Force relaxation experiments during contact of the tip on
213the oocyst and the superposition of trace and retrace parts of the force curves indicated
214that no viscous behavior could be identified in this range of stimulations (Fig. 3A,B). In
215addition, repetitions of contacts lead to rather unvarying indentation depths, with no
216apparent tendency of any plastic deformation of the oocyst wall for the investigated
217forces (Fig. 3C).

218Pressing the oocysts at higher forces (30 or 120 nN) did not appear to strongly modify the
219mechanics of the oocyst wall (*SI Appendix*, Fig. S5F,G). However, in these conditions,
220we observed that oocysts were accidentally removed from the slide because of the higher
221pressing force, making the AFM tip into a golf club and the oocyst the ball.

222

223**Adhesive Properties of the Oocyst Wall.** In addition to indentation and elasticity
224measurements, the non-specific adhesive properties of the oocyst wall were examined.
225Surface adhesion (Fig. 4) was measured as the force required to detach the AFM tip from
226the surface of the oocyst after indentation at 1 nN, with a fixed pulling speed of 1 μ m/s.

227We observed that at least 50% of the force curves showed some adhesion (Fig. 4A vs.
228Fig 4B). The proportion of oocysts showing a detectable adhesion was observed to
229depend on the developmental stage and on the treatment of the oocyst surface.
230Temperature alone lowered the proportion of oocysts with adhesive surface properties
231while application of bleach increased it (Fig. 4C and D). Upon repeated pulling on the
232same object, adhesive forces did not show any marked tendency (Fig. 4E) indicating that
233materials coming from the wall did not pollute the tip. We observed that the strength of
234adhesion (i.e. the force required to fully detach the tip from the oocyst) was rather low
235(<100 pN) for control and temperature-treated oocysts but was significantly stronger
236when bleach was applied as a first treatment (Fig. 4F and *SI Appendix*, Table S3)
237suggesting important bleach-induced modifications of the wall. In conclusion, bleach
238treatment increases both the proportion of oocysts showing detectable adhesion and the
239overall strength of the adhesion while high temperature treatment alone did not affect
240adhesion force but reduces the proportion of oocysts showing significant adhesion.

241

242Discussion

243The *T. gondii* oocyst is a superstructure that protects the dormant but potentially infective
244sporozoites from many extreme conditions that would be deleterious for survival (24).
245Facing the external environment, the oocyst wall acts as a primary barrier to physical and
246chemical attacks as long as its complex polymeric organization is perfectly maintained
247(8, 12, 26). Different, but complementary, approaches have been applied to investigate
248the structure and molecular basis of the oocyst wall resilience, such as electronic
249microscopy (9, 12, 24, 51) and proteomics studies (10, 12). However, oocysts are

250technically difficult to process for electron microscopy examination because of the
251impervious nature of the walls and proteomics usually require large numbers of highly
252purified oocysts, which are difficult to obtain since oocysts cannot be generated in vitro.
253Here, we addressed the structure and chemistry of each oocyst wall layer by measuring
254their respective mechanical properties by combining wall treatments, fluorescence and
255electron microscopic observations, and AFM techniques on immobilized parasites.
256In coccidian parasites such as *T. gondii*, the oocyst wall results from the particular
257arrangement of structural proteins through a sclerotization process involving both
258quinone tanning and protein dityrosine crosslinking and dehydration (12, 26). This
259process probably takes place very early in the development of the oocyst wall, from the
260NS stage before it leaves the host (21), and is thought to lead to hardened structures,
261which excludes water-soluble molecules in order to form a complex polymeric covering
262capable of resisting extended physical and chemical-induced disorganization.
263Interestingly, it has been recently claimed that the inner wall layer of *Eimeria tenella*
264oocysts possesses discrete pores of 5-250 nm (9). However, such structures in the *T.*
265*gondii* oocyst wall were not observed in the present or previous studies (26).
266The oocyst wall layers in *T. gondii* are assumed to differ in their thickness and molecular
267content, the inner one being thicker, less electron dense and more resistant to chemical
268degradation than the outer one (8). Using fluorescence imaging and electron microscopy
269combined with different treatments, we provide new insights on the structure and
270chemistry of the wall of *T. gondii* oocysts. Specific immuno-staining of the inner wall
271layer of H₂O-exposed oocysts was infrequent and appeared to result from the infiltration
272of the antibody through focal openings of the oocyst wall rather than exposure of the

273external surface of the inner layer. After heating, antibody staining was significantly
274decreased in control oocysts while it had little, if no, effect on bleach-treated oocysts.
275This would suggest that heating is not denaturing the antigen recognized by the antibody
276and probably results from heat-induced reticulation of poly-protein structures of the outer
277layer reducing penetration of the antibody. In contrast, bleach treatment clearly affected
278both the structure and chemistry of the oocyst wall, by removing the outer layer as seen
279in our EM micrographs and significantly affecting the oocyst wall AF. Consequently,
280most of the 4B6 staining observed in bleached oocysts could be linked to the exposure of
281the external surface of the inner layer of the oocyst wall.

282Then, we investigated the mechanical properties of the double-layered oocyst wall, and
283then those specific to the inner layer after removing the outer layer by treatment with
284bleach. We observed high *E* moduli comparable to polymeric shells (50) with neither
285viscous nor plastic behaviors. The *E* moduli were not significantly different between the
286different maturing stages and treatments involving temperature and bleach (alone or in
287combination). Considering the small indentation and high *E* modulus, our results strongly
288support that the global stiffness of the bilayered oocyst wall is in the same order as that of
289the inner layer alone. Interestingly, we showed that the oocyst wall stiffness did not vary
290significantly following parasite incubation at 80°C, which was quite unexpected since
291heat-induced stresses usually result in increasing stiffness of polymeric multilayer
292microcapsules due to an increased shell thickness or reticulation (52). The conservative
293hypothesis suggests that each wall layer retains its basic mechanical properties by
294maintaining to large extend its molecular architecture, even at this temperature.

295 Besides mechanical measurements, AFM has also permitted examination of the non-
296 specific adhesive properties of each layer of the wall. It was observed that the proportion
297 of oocyst showing adhesive properties was lower as was the strength of the adhesion (i.e.
298 overall force needed to fully detach the tip from the oocyst) in parasites retaining their
299 typical double-layered wall structure, whereas there was a higher proportion of oocysts
300 with adhesive properties and stronger adhesion was recorded in oocysts exposing solely
301 the inner wall layer (*SI Appendix*, Fig. S6). This contrasting behavior might indicate the
302 existence of important differences regarding the biochemical nature of the molecules
303 and/or their arrangement from one wall layer to the other resulting from oocyst
304 treatments modulating the structure of the wall. We speculate an increasing number of
305 residual polypeptidic chains due to removal of (most of, if not all) the most outer layer of
306 the wall (*SI Appendix*, Fig. S6). Such differences have also been hypothesized by others
307 (10), based on proteomics analyses of purified wall fractions of *T. gondii* oocysts exposed
308 or not to bleach. It is not yet clear whether these different adhesive properties play a role
309 in the oocyst fate. Recent studies have shown that the negative charges covering the
310 surface of the oocyst wall prevent in most cases any aggregation of the parasites with
311 other particles, thus allowing the parasites to disperse freely in fresh water (8). Further
312 investigations, in particular on molecule-specific adhesion and the effects of digestive
313 enzymes found in the host's gut, are required to extend our study and refine the biological
314 significance of the adhesive properties of the oocyst wall.

315 From a methodological point of view, this study proposes a simple but efficient way to
316 immobilize hardened biological microparticles such as *T. gondii* oocysts on glass slides
317 for investigating the biophysical properties of their multilayer wall by using AFM and

318fluorescence microscopy techniques. It opens the possibility to extend such studies to
319immobilized *T. gondii* sporocysts and to other environmentally-resistant parasitic
320pathogens such as *Cryptosporidium* and *Giardia* (53–56).

321In conclusion, our study demonstrates that the overall rigidity of the bilayered *T. gondii*
322oocyst wall is as high as common plastic materials and that the inner layer is as robust as
323the bilayered wall itself. These findings strongly suggest that the mechanical
324characteristics of the *T. gondii* oocyst wall sustain the survival of the enclosed
325sporozoites facing physical and chemical attacks outside the host. In particular, our
326results suggest that chlorine-based products used as surface disinfectants or for treating
327drinking water are ineffective for efficiently killing *T. gondii* oocysts because these
328compounds are not able to permeabilize or disrupt the oocyst wall. However, it is clear
329that these properties have to be circumvented following oocyst ingestion by the host, in
330order to safely deliver the sporozoites near the enterocytes. As chemicals are ineffective
331in breaking the oocyst wall, a supplementary physical stimulus (still to be determined)
332seems to be required to prime oocyst-related infections in humans and animals.

333

334Materials and Methods

335**Oocyst Purification and Sporulation.** Oocysts of the genotype II TgNmBr1strain of *T.*
336*gondii* (57) were harvested from feces of cat 6-8 days after feeding infected mouse tissues
337to a *T. gondii* free cat (1), then purified by flotation, and allowed to sporulate at RT for 5
338days. More details can be found in SI. Oocyst suspension was stored in distilled water at
3394°C until used within 3 months. More details can be found in *SI Appendix*.

340

341 **Chemical and Physical Treatment of the Oocysts**

342 **Bleach Treatment.** H₂O-stored oocysts were washed three times in PBS at 5000g 5 min
343 and then incubated with 1 mL of bleach solution containing 3% sodium hypochlorite
344 (Fouque Chimie Service, Marseille, France) in PBS for 30 min at 4°C. The oocysts were
345 then washed three times in PBS to remove bleach prior to be immobilized on coverslips
346 for AFM experiments.

347 **Heat Inactivation.** H₂O-stored or bleach-treated oocysts were washed three times in PBS
348 at 5000 g for 5 min, resuspended in 500 µL PBS and then placed in a dry block heater for
349 10 min at 80°C to allow their inactivation prior to AFM experiments.

350

351 **Electron Microscopy.** Samples of water maintained and bleached oocysts were mechan-
352 ically ruptured prior to fixation in 2.5% glutaraldehyde in 0.1M phosphate buffer and
353 processed for routine electron microscopy. In summary, the samples were post-fixed in
354 osmium tetroxide, dehydrated in ethanol, treated with propylene oxide and embedded in
355 Spurr's epoxy resin. Thin sections were cut and stained with uranyl acetate and lead cit-
356 rate prior to examination in a Jeol 1200EX electron microscope.

357

358 **Immunofluorescence Assay (IFA).** The effects of bleach and heat treatments on the
359 integrity of the oocyst wall were evaluated by IFA combined with the autofluorescent
360 signal (AF). We labeled oocysts in suspension using a monoclonal antibody (IgM mAb
361 4B6), which was previously shown to react mainly with the inner layer of the oocyst wall
362 (49, 58). More details can be found in *SI Appendix*.

363

364**FITC Infiltration Assay.** The permeability of the wall of oocysts exposed or not to
365bleach treatment was assessed by incubating oocysts with FITC at 0.5 mg/mL in PBS for
3661 hr at room temperature. Oocysts were subsequently washed four times in PBS by gentle
367centrifugations at 5000 g for 5 min and examined for fluorescence of FITC bound to
368internal proteins (*SI Appendix*, Fig. S3).

369

370**Measurements of the Oocyst Wall Autofluorescence Intensity.** The effects of bleach
371treatment on the autofluorescence pattern of the oocyst wall were evaluated on AF gray
372scale images as described in *SI Appendix*, Fig. S4.

373

374**AFM Experiments**

375**Oocyst Immobilization on Glass Coverslides.** Clean glass coverslides were coated with
376poly-L-lysine (PLL) after activation using a residual air-based plasma. After rinsing and
377mounting on an observation chamber, a diluted suspension of untreated, heat-inactivated,
378or bleach-treated oocysts was seeded onto the PLL treated zone and let to settle for 45min
379to 1 hr at RT before removal of non adherent objects. We observed that this procedure
380did not grossly affect the different sub-populations ratios as compared to the original
381suspension (*SI Appendix*, Fig. S5B). More details can be found in *SI Appendix*.

382**AFM Measurements.** A Nanowizard I (JPK Instruments, used in closed loop mode)
383sitting on an Axiovert 200 (Zeiss) equipped with 10x and 40x lenses (with an optional
3841.6x lens) was used to measure the oocyst mechanics. The system was sitting on an active
385damping table (Halcyonics) to suppress mechanical noise. Blunt AFM levers (MLCT,
386Veeco, nominal spring constant 10 pN/nm) were used and calibrated in situ. The spring

387constant ($\sim 15\text{-}18$ pN/nm) was determined in situ using a built-in thermal calibration
388method, far from the glass surface to avoid any hydrodynamical bias due to the coupling
389with the substrate (59).

390Using bright field, a given oocyst was chosen and a calibrated AFM cantilever was
391positioned on top of it (*SI Appendix*, Fig. S5C,D). We checked that the measurements
392were not affected by the fine positioning of the tip on top of the structures (e.g. over the
393two substructures of SP oocysts and between them, so only the mid position was used to
394quantify the structure's mechanics (*SI Appendix*, Fig. S5D,E).

395At least 10 force curves, with a preset contact force of 1 nN, a preset contact time of 0
396sec, pressing/pulling speeds of 1 $\mu\text{m/sec}$ and an acquisition frequency of 1024 Hz, were
397acquired per oocyst (Fig. 3A,B). Each force curve was evaluated by eye and processed on
398a PC using the built-in JPK IP software (JPK Instruments), resulting in 3 to more than 15
399data points extracted for each structure. We first observed that the maximal indentation
400depth at 1 nN was in average ~ 20 nm (Fig. 3C,D), that is less than the thickness of the
401bilayered wall structure, so the model was accurate enough to allow us to extract the
402Young modulus of the structures, E , one per valid force curve. To quantify the
403mechanics, we used as a first approximation a Hertz model for contact to fit the pressing
404part of the force curves assuming a pyramidal tip of $\alpha=21^\circ$ half angle (calculated from
405manufacturer data) and incompressibility of the material ($\nu=0.5$) (37) (Fig. 3A,B). Since
406the indentation was <50 nm, we also tried the Hertz model for a spherical indenter of 25-
40750 nm radius and found little differences in the quality of the fit and subsequently
408calculated E moduli.

409For adhesion measurements, we retrieved from the return/pulling part of the force curves

410the maximum detachment force (Fig. 4B) and frequency of adhesion events (i.e. the ratio
411between the number of force curves having adhesion divided by the total number of force
412curves taken into account) (Fig 4C,D). We then calculated median adhesion forces and
413plotted the entire force distribution as whisker plots. We did not observe any tendency of
414adhesion force versus upon repetitions of tests (Fig. 4E).

415Experiments lasted maximum 2 hr at RT before changing the sample and the cantilever
416with occasional supplementations of water to counteract the evaporation.

417

418**Data Processing and Statistical Analysis**

419The distributions of the pooled data being non gaussian, median values with data points
420and/or whisker plots were then plotted as a function of the oocyst stage and treatment
421using Prism 5.0 and 6.0 (GraphPad). The data sets were compared using non-parametric
422tests such as Kruskal-Wallis.

423

424**Acknowledgments**

425We gratefully thank M.L. Dardé (INSERM U 1094 NET, Limoges University, France)
426for providing 4B6 hybridoma, and P.A.R.I.S. Biotech (Compiègne, France) for antibody
427production and purification. This work was supported by Aix-Marseille University
428(Préciput 2011 program). A.D. and N.A. are currently supported by the ANR Protofood
429program, and P.-H.P. by the ANR JCJC DissecTion program.

430

431**Author contributions**

432 A.D. and P.-H.P. designed research; A.D., J.P.D., D.J.P.F. and P.-H.P. performed
433 research; A.D., J.P.D., D.J.P.F., P.B., N.A. and P.-H.P. contributed
434 reagents/materials/analysis tools; A.D., J.P.D., D.J.P.F. and P.-H.P. analyzed the data, and
435 A.D., J.P.D., D.J.P.F. and P.-H.P. wrote the paper.

436

437 **References**

4381. Dubey J (2010) *Toxoplasmosis of animals and humans*. Second edition (CRC Press),
439 pp 1-313.

4402. Bahia-Oliveira LMG et al. (2003) Highly endemic, waterborne toxoplasmosis in
441 north Rio de Janeiro state, Brazil. *Emerging Infect Dis* 9:55–62.

4423. De Moura L et al. (2006) Waterborne toxoplasmosis, Brazil, from field to gene.
443 *Emerging Infect Dis* 12:326–329.

4444. Jones JL, Dubey JP (2010) Waterborne toxoplasmosis-recent developments. *Exp*
445 *Parasitol* 124:10–25.

4465. Boyer K et al. (2011) Unrecognized ingestion of *Toxoplasma gondii* oocysts leads to
447 congenital toxoplasmosis and causes epidemics in North America. *Clin Infect Dis*
448 53:1081–1089.

4496. Dattoli VCC et al. (2011) Oocyst ingestion as an important transmission route of
450 *Toxoplasma gondii* in Brazilian urban children. *J Parasitol* 97:1080–1084.

4517. Robert-Gangneux F, Dardé M-L (2012) Epidemiology of and diagnostic strategies for
452 toxoplasmosis. *Clin Microbiol Rev* 25:264–296.

4538. Dumètre A et al. (2012) Interaction forces drive the environmental transmission of
454 pathogenic protozoa. *Appl Environ Microbiol* 78:905–912.

4559. Bushkin GG et al. (2012) β -1,3-glucan, which can be targeted by drugs, forms a
456 trabecular scaffold in the oocyst walls of *Toxoplasma* and *Eimeria*. *mBio* 3:e00258-
457 12.

45810. Fritz HM, Bowyer PW, Bogyo M, Conrad PA, Boothroyd JC (2012) Proteomic
459 analysis of fractionated *Toxoplasma* oocysts reveals clues to their environmental
460 resistance. *PLoS ONE* 7:e29955.

46111. Fritz HM et al. (2012) Transcriptomic analysis of *Toxoplasma* development reveals
462 many novel functions and structures specific to sporozoites and oocysts. *PLoS ONE*
463 7:e29998.

46412. Mai K et al. (2009) Oocyst wall formation and composition in coccidian parasites.
465 *Mem Inst Oswaldo Cruz* 104:281–289.

46613. Possenti A et al. (2010) Molecular characterisation of a novel family of cysteine-rich
467 proteins of *Toxoplasma gondii* and ultrastructural evidence of oocyst wall
468 localisation. *Int J Parasitol* 40:1639–1649.

46914. Dumètre A et al. (2008) Effects of ozone and ultraviolet radiation treatments on the
470 infectivity of *Toxoplasma gondii* oocysts. *Vet Parasitol* 153:209–213.

47115. Wainwright KE et al. (2007) Chemical inactivation of *Toxoplasma gondii* oocysts in
472 water. *J Parasitol* 93:925–931.

47316. Wainwright KE et al. (2007) Physical inactivation of *Toxoplasma gondii* oocysts in
474 water. *Appl Environ Microbiol* 73:5663–5666.

47517. Villegas EN et al. (2010) Using quantitative reverse transcriptase PCR and cell
476 culture plaque assays to determine resistance of *Toxoplasma gondii* oocysts to
477 chemical sanitizers. *J Microbiol Methods* 81:219–225.

47818. Ware MW et al. (2010) Determining UV inactivation of *Toxoplasma gondii* oocysts
 479 by using cell culture and a mouse bioassay. *Appl Environ Microbiol* 76:5140–5147.

48019. Dubey JP, Frenkel JK (1972) Cyst-induced toxoplasmosis in cats. *J Protozool*
 481 19:155–177.

48220. Ferguson DJ, Hutchison WM, Dunachie JF, Siim JC (1974) Ultrastructural study of
 483 early stages of asexual multiplication and microgametogony of *Toxoplasma gondii* in
 484 the small intestine of the cat. *Acta Pathol Microbiol Scand B Microbiol Immunol*
 485 82:167–181.

48621. Ferguson DJ, Hutchison WM, Siim JC (1975) The ultrastructural development of the
 487 macrogamete and formation of the oocyst wall of *Toxoplasma gondii*. *Acta Pathol*
 488 *Microbiol Scand B* 83:491–505.

48922. Dubey JP, Miller NL, Frenkel JK (1970) The *Toxoplasma gondii* oocyst from cat
 490 feces. *J Exp Med* 132:636–662.

49123. Ferguson DJ, Birch-Andersen A, Siim JC, Hutchison WM (1979) Ultrastructural
 492 studies on the sporulation of oocysts of *Toxoplasma gondii*. III. Formation of the
 493 sporozoites within the sporocysts. *Acta Pathol Microbiol Scand B* 87:253–260.

49424. Speer CA, Clark S, Dubey JP (1998) Ultrastructure of the oocysts, sporocysts, and
 495 sporozoites of *Toxoplasma gondii*. *J Parasitol* 84:505–512.

49625. Dumètre A, Dardé ML (2003) How to detect *Toxoplasma gondii* oocysts in
 497 environmental samples? *FEMS Microbiol Rev* 27:651–661.

49826. Belli SI, Smith NC, Ferguson DJP (2006) The coccidian oocyst: a tough nut to crack!
 499 *Trends Parasitol* 22:416–423.

50027. Dubey JP (1998) *Toxoplasma gondii* oocyst survival under defined temperatures. *J*
501 *Parasitol* 84:862–865.

50228. Belli SI, Wallach MG, Luxford C, Davies MJ, Smith NC (2003) Roles of tyrosine-
503 rich precursor glycoproteins and dityrosine- and 3,4-dihydroxyphenylalanine-
504 mediated protein cross-linking in development of the oocyst wall in the coccidian
505 parasite *Eimeria maxima*. *Eukaryotic Cell* 2:456–464.

50629. Lindquist HDA et al. (2003) Autofluorescence of *Toxoplasma gondii* and related
507 coccidian oocysts. *J Parasitol* 89:865–867.

50830. Franz C, Puech P-H (2008) Atomic Force Microscopy: A versatile tool for studying
509 cell morphology, adhesion and mechanics. *Cell Mol Bioeng* 1:289–300.

51031. Muller DJ, Dufrêne YF (2011) Force nanoscopy of living cells. *Curr Biol* 21:R212–
511 R216.

51232. Muller DJ, Krieg M, Alsteens D, Dufrêne YF (2009) New frontiers in atomic force
513 microscopy: analyzing interactions from single-molecules to cells. *Curr Opin*
514 *Biotechnol* 20:4–13.

51533. Müller DJ, Dufrêne YF (2008) Atomic force microscopy as a multifunctional
516 molecular toolbox in nanobiotechnology. *Nat Nanotechnol* 3:261–269.

51734. Friedrichs J, Taubenberger A, Franz CM, Muller DJ (2007) Cellular remodelling of
518 individual collagen fibrils visualized by time-lapse AFM. *J Mol Biol* 372:594–607.

51935. Muller DJ (2008) AFM: a nanotool in membrane biology. *Biochemistry* 47:7986–
520 7998.

52136. Müller DJ et al. (2006) Single-molecule studies of membrane proteins. *Curr Opin*
522 *Struct Biol* 16:489–495.

52337. Radmacher M (2002) Measuring the elastic properties of living cells by the atomic
524 force microscope. *Methods Cell Biol* 68:67–90.

52538. Radmacher M (2007) Studying the mechanics of cellular processes by atomic force
526 microscopy. *Methods Cell Biol* 83:347–372.

52739. Milosavljevic N et al. (2010) Nongenomic effects of cisplatin: acute inhibition of
528 mechanosensitive transporters and channels without actin remodeling. *Cancer Res*
529 70:7514–7522.

53040. Hampoelz B et al. (2011) Microtubule-induced nuclear envelope fluctuations control
531 chromatin dynamics in *Drosophila* embryos. *Development* 138:3377–3386.

53241. Puech P-H, Poole K, Knebel D, Muller DJ (2006) A new technical approach to
533 quantify cell-cell adhesion forces by AFM. *Ultramicroscopy* 106:637–644.

53442. Fierro FA et al. (2008) BCR/ABL expression of myeloid progenitors increases beta1-
535 integrin mediated adhesion to stromal cells. *J Mol Biol* 377:1082–1093.

53643. Taubenberger A et al. (2007) Revealing early steps of alpha2beta1 integrin-mediated
537 adhesion to collagen type I by using single-cell force spectroscopy. *Mol Biol Cell*
538 18:1634–1644.

53944. Franz CM, Taubenberger A, Puech P-H, Müller DJ (2007) Studying integrin-
540 mediated cell adhesion at the single-molecule level using AFM force spectroscopy.
541 *Science's STKE* 2007:pl5–pl5.

54245. Puech P-H et al. (2011) Force measurements of TCR/pMHC recognition at T cell
543 surface. *PLoS ONE* 6:e22344.

54446. Puech P-H et al. (2005) Measuring cell adhesion forces of primary gastrulating cells
545 from zebrafish using atomic force microscopy. *J Cell Sci* 118:4199–4206.

54647. Ulrich F et al. (2005) Wnt11 functions in gastrulation by controlling cell cohesion
547 through Rab5c and E-cadherin. *Dev Cell* 9:555–564.

54848. Ferguson DJ, Birch-Andersen A, Siim JC, Hutchison WM (1979) Ultrastructural
549 studies on the sporulation of oocysts of *Toxoplasma gondii*. I. Development of the
550 zygote and formation of the sporoblasts. *Acta Pathol Microbiol Scand B* 87B:171–
551 181.

55249. Dumètre A, Dardé M-L (2007) Detection of *Toxoplasma gondii* in water by an
553 immunomagnetic separation method targeting the sporocysts. *Parasitol Res* 101:989–
554 996.

55550. Dubreuil F, Elsner N, Fery A (2003) Elastic properties of polyelectrolyte capsules
556 studied by atomic-force microscopy and RICM. *Eur Phys J E Soft Matter* 12:215–
557 221.

55851. Dubremetz JF, Ferguson DJP (2009) The role played by electron microscopy in
559 advancing our understanding of *Toxoplasma gondii* and other apicomplexans. *Int J*
560 *Parasitol* 39:883–893.

56152. Delcea M et al. (2010) Mechanobiology: correlation between mechanical stability of
562 microcapsules studied by AFM and impact of cell-induced stresses. *Small* 6:2858–
563 2862.

56453. Byrd TL, Walz JY (2005) Interaction force profiles between *Cryptosporidium*
565 *parvum* oocysts and silica surfaces. *Environ Sci Technol* 39:9574–9582.

56654. Byrd TL, Walz JY (2007) Investigation of the interaction force between
567 *Cryptosporidium parvum* oocysts and solid surfaces. *Langmuir* 23:7475–7483.

56855. Considine RF, Dixon DR, Drummond CJ (2002) Oocysts of *Cryptosporidium*
569 *parvum* and model sand surfaces in aqueous solutions: an atomic force microscope
570 (AFM) study. *Water Res* 36:3421–3428.

57156. Considine R, Dixon D, Drummond C Laterally-resolved force microscopy of
572 biological microspheres-oocysts of *Cryptosporidium parvum*. *Langmuir* 16:1323–
573 1330.

57457. Dubey JP et al. (2011) Isolation of viable *Toxoplasma gondii* from feral guinea fowl
575 (*Numida meleagris*) and domestic rabbits (*Oryctolagus cuniculus*) from Brazil. *J*
576 *Parasitol* 97:842–845.

57758. Dumètre A, Dardé M-L (2005) Immunomagnetic separation of *Toxoplasma gondii*
578 oocysts using a monoclonal antibody directed against the oocyst wall. *J Microbiol*
579 *Methods* 61:209–217.

58059. Butt H-J, Jaschke M (1995) Calculation of thermal noise in atomic force microscopy.
581 *Nanotechnology* 6:1–7.

582
583

584 **Figure Legends**

Figure 1: Ultrastructure of the *T. gondii* oocyst wall. (A) Low magnification image of a control (water maintained) oocyst showing the ruptured oocyst wall (OW) and the remnants of a sporocyst (Sp). Bar is 1 μ m. (B) Detail of the oocyst wall from a control oocyst showing the thinner outer layer (O) and the thicker inner layer (I). Bar is 100 nm. (C) Detail of the oocyst wall from a bleached oocyst showing the inner layer (I) with loss of the outer layer except for a few remnants (arrows). Bar is 100 nm. (D) Detail of the sporocyst wall from a control oocyst showing the outer (O) and inner (I) layers of the wall. Bar is 100 nm. (E) Detail of the sporocyst wall from a bleached oocyst showing the retention of both the outer (O) and inner (I) layers for the wall. Bar is 100 nm.

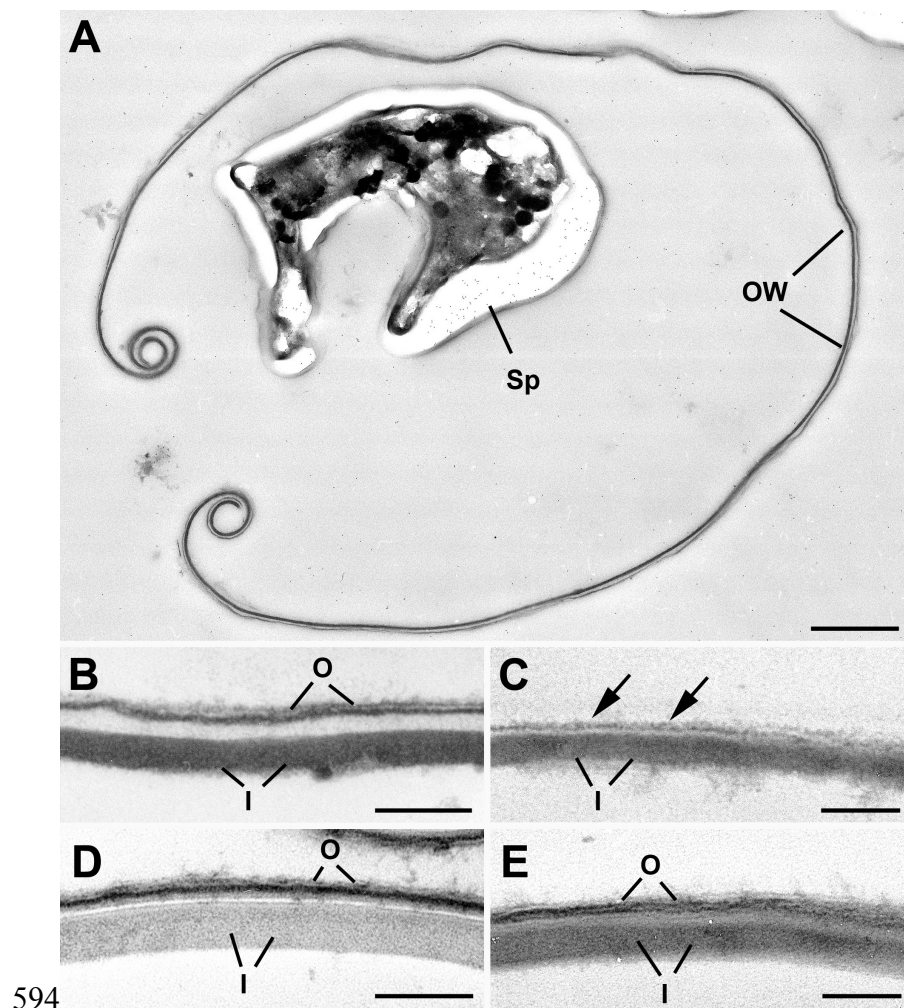
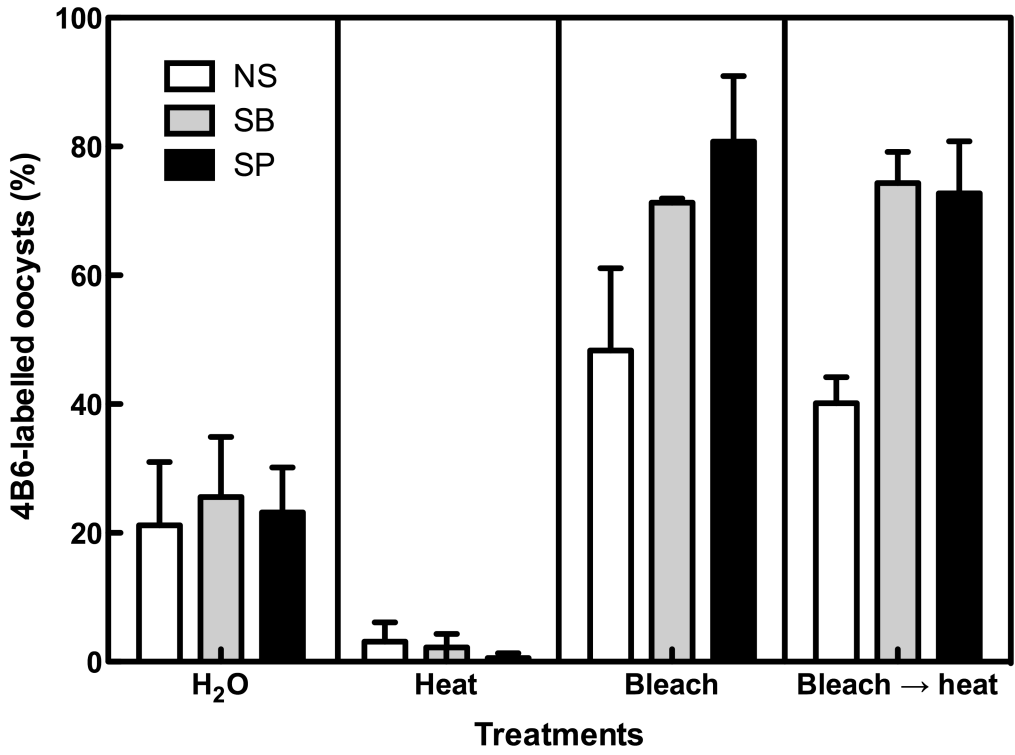


Figure 2: Fluorescence labeling of the inner wall of *T. gondii* oocysts submitted to different surface treatments. Non sporulated (NS), sporoblast-staged (SB) and sporulated (SP) oocysts were bleached and/or heated prior to be allowed to react with 4B6 antibody specific to their inner wall (49, 58). The percentages of labeled parasites in each treatment condition are presented. No significant differences were observed between the stages of oocyst maturation for any given treatment. However there were significant differences among treatments, with control H₂O oocysts differing from heated, bleached, and bleached then heated oocysts (p values <0.001-0.05) and heated oocysts differing from bleached, and bleached then heated oocysts (p<0.001). No statistical difference was noted between bleached oocysts and bleached then heated oocysts at any maturing stage. The corresponding typical fluorescence images are presented on *SI Appendix*, Fig. S2.

606

607



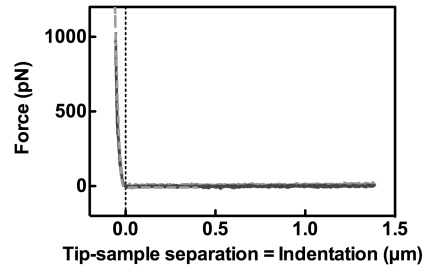
608

609

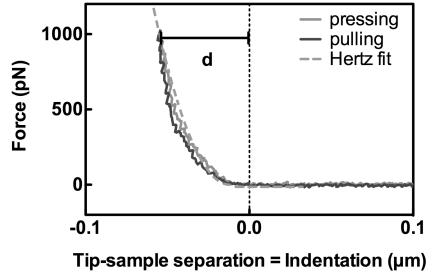
Figure 3: Measuring mechanical properties of *T. gondii* oocysts. (A) Typical force curve (Force vs. Tip-sample separation) used for quantifying the Young modulus (note that pressing and pulling curves are almost superimposed). The dotted line is the point of contact. (B) Zoom on the contact region of the curves presented in A, showing the superimposition of pressing and pulling curves together with the Hertz fit described in the text (dotted line), and d the maximal indentation. The superimposition of pressing and pulling curves shows that little if no dissipation is occurring in the material when indenting, ruling out any viscoelastic behavior under the conditions of our experiments. (C) Example of maximal indentation for untreated oocysts of different subtypes, showing no tendency upon repeated indentation. Note that 100 nm was used as the maximum of the scale as it is the upper bound of the thickness of the oocyst wall found in literature. (D) Maximal indentation under a force of 1 nN as a function of oocyst subtype and treatment. (E) Repeated measured values of Young modulus of 3 untreated oocysts of various subtypes, showing that for a given object no tendency can be observed upon repeated indentation. Note that the value of 10^4 Pa used as the lower limit of the scale corresponds to the values recorded for hard eukaryotic cells as found in literature. (F) Young modulus as a function of oocyst subtype and treatment. In D and F, each point is the median value obtained for a single oocyst upon successive indentations. The line is the median of the subsequent distribution. No significant differences are observed between the conditions neither for indentation (D and *SI Appendix*, Tables S1, S4) nor for Young modulus (F and *SI Appendix*, Tables S2, S4).

631

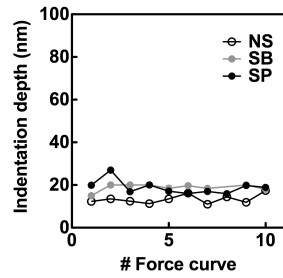
A



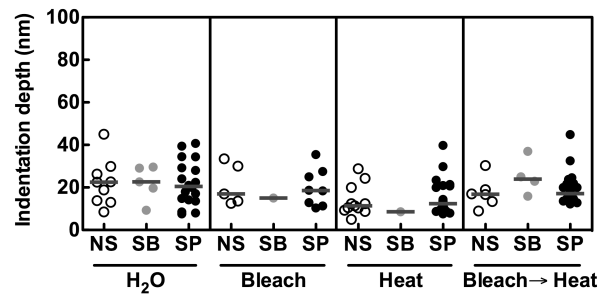
B



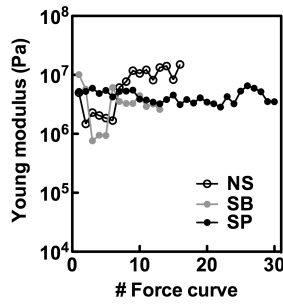
C



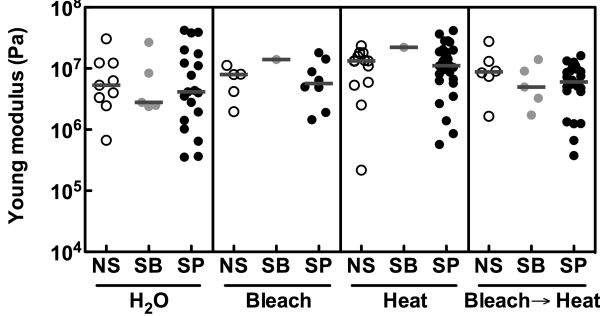
D



E

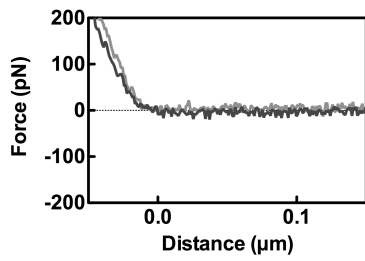
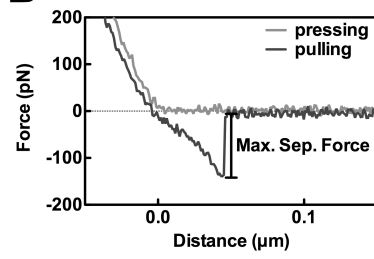
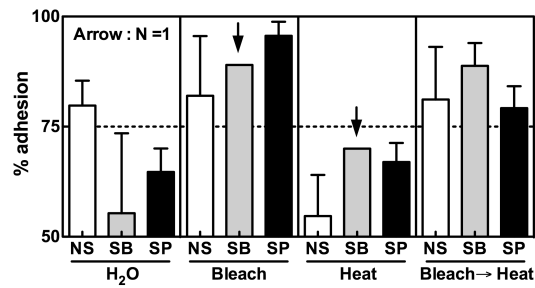
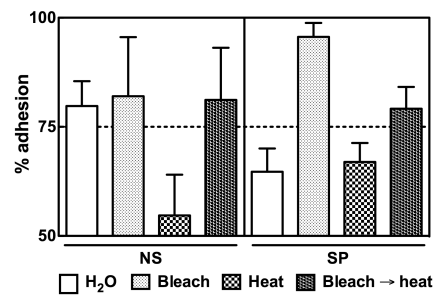
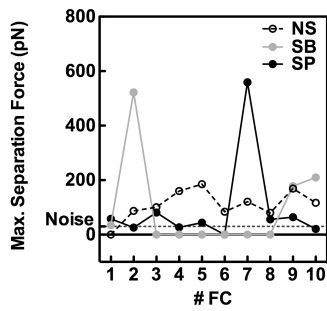
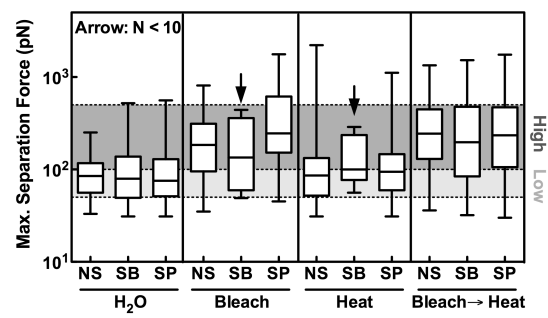


F



632

Figure 4: Measuring non-specific adhesive properties of *T. gondii* oocysts. (A) Typical force curve showing no adhesion event. (B) Typical force curve showing adhesion event. We present here the zoom on the force curve near the contact / adhesion zone, with the recorded maximal adhesion force. Note that the noise is far below the forces measured (typically 15 to 30 pN). (C) The fraction of adhesion as a function of oocyst subtypes and treatments (mean +/- SD over the different days of experiments). Arrows show cases where only one object for a given condition was observed over different repetitions. Dotted line has been placed at 75 % adhesion as a guide for the eye. (D) Same data as in C, showing the comparison of NS and SP oocysts as a function of treatment. (E) Example of maximal separation force for untreated oocysts of different subtypes, showing no tendency upon repeated indentation / pulling, indicating that no strong pollution of, or transfer of material, to the lever tip was observed. Note that the dotted line corresponds to the average observed noise on the baseline of the force curves. (F) Distribution of adhesion forces as whisker plots for oocysts of different subtypes and treatments. The significant differences correspond to the high / low adhesion separation on the graph (*SI Appendix*, Tables S3 and S4).

A**B****C****D****E****F**

651

652

653 *Supplement Information (SI) Appendix*

654

655 **Materials and Methods**

656

657 **Oocyst Purification and Sporulation.** Oocysts of the genotype II TgNmBr1 strain of *T.*
658 *gondii* (1) were harvested from feces of cat 6-8 days after feeding infected mouse tissues
659 to a *T. gondii* free cat. Oocysts were collected by flotation at 4°C from cat feces on a 1.15
660 specific gravity sucrose solution without phenol. Concentrated oocyst pellets were then
661 resuspended in 5 mL of distilled water and sent with cold packs within 48 hours by
662 FedEx from Beltsville, Maryland, USA to Marseille, France, for sporulation and further
663 experiments. Upon arrival, oocysts were washed three times in distilled water, pelleted by
664 centrifugation at 5000 g for 5 min at room temperature (RT, 20-22°C), then resuspended
665 in 7 mL of distilled water, and transferred in a 100 mL small plastic container. Oocysts
666 were allowed to sporulate at RT for 5 days under adequate aeration and gentle continuous
667 shaking. Sporulation progress was monitored daily by examining a fraction of the
668 suspension by using bright field and UV microscopy as described elsewhere (2, 3).
669 Oocyst suspension was stored in distilled water at 4°C until used within 3 months.

670

671 **Immunofluorescence Assay (IFA).** The effects of bleach and heat treatments on the
672 integrity of the oocyst wall were evaluated by IFA combined with the autofluorescent
673 signal (AF). We used a monoclonal antibody (IgM mAb 4B6), which was previously
674 shown to react mainly with the inner layer of the oocyst wall (4, 5). This labeling was
675 performed on oocysts in suspension rather than on air-dried parasites because drying on
676 slides frequently induces the opening of the oocyst wall, which invariably gives to the
677 mAb 4B6 an access to the inner layer (4, 5).

678 Briefly, untreated (H₂O-stored), heat-inactivated and bleach-treated oocysts were allowed
679 to react with mAb 4B6 diluted at 1:100 in PBS for 30 min at 37°C. Oocysts were
680 subsequently washed three times in PBS by gentle centrifugations at 5000 g for 5 min
681 prior to incubation with a goat fluorescein-isothiocyanate (FITC) conjugate anti-mouse
682 IgM+IgG (50-011, Argene, France) diluted to 1:100 in PBS. After that, parasites were
683 washed again three times in PBS using the same protocol. Samples are then mounted and

684examined on a BX51 microscope (Olympus, France) equipped with suitable
685epifluorescence filters for FITC and UV autofluorescence (AF) and 40x lens. Bright field,
686FITC and AF images were acquired using the fluorescence imaging system Cell^A
687(Olympus, France) and quantified using ImageJ 1.46m. The normally blue AF signal
688(Fig. S1B) was placed in the red channel and the FITC in the green channel for more
689convenient merging when performing fluorescence colocalization (Fig. S2).

690

691**Oocyst Immobilization on Glass Coverslides.** Coverslides were cleaned using a 10%
692v/v Helmanex (Helma) solution in water in an ultrasonic bath for 30 min at 60°C,
693subsequently separately rinsed using alternating baths of ethanol and MQ water (three of
694each). Then, a supplementary cleaning in MQ water in an ultrasonic bath for 30 min at
69560°C was performed before a last rinsing step with MQ water prior to drying under an air
696flow. Coverslides were stored away from humidity and dust for up to two weeks before
697use. For coating with poly-L-lysine (PLL), clean coverslides were activated for 1 min
698using a residual air-based plasma cleaner and a PDMS stamp with a circular 8 mm in
699diameter hole was stuck on them. 100 µL of 0.01% PLL in water was added and
700incubated for 45 min to 1 hr at RT. Three rinsing with PBS were performed before gluing
701a plastic ring with vacuum grease after removal of the PDMS stamp. The resulting
702chamber was then filled with 1 mL PBS and 100 µL of untreated, heat-inactivated, or
703bleach-treated oocyst suspension were seeded onto the PLL treated zone and let to settle
704for 45min to 1 hr at RT. Three gentle rinsing steps, with 1mL PBS, were performed
705before mounting on the AFM. We observed that this procedure did not grossly affect the
706different sub-populations ratios as compared to the original suspension (Fig. S5B).
707Observation lasted for 2 hr maximum at RT with occasional supplementations of water to
708counteract the evaporation.

709

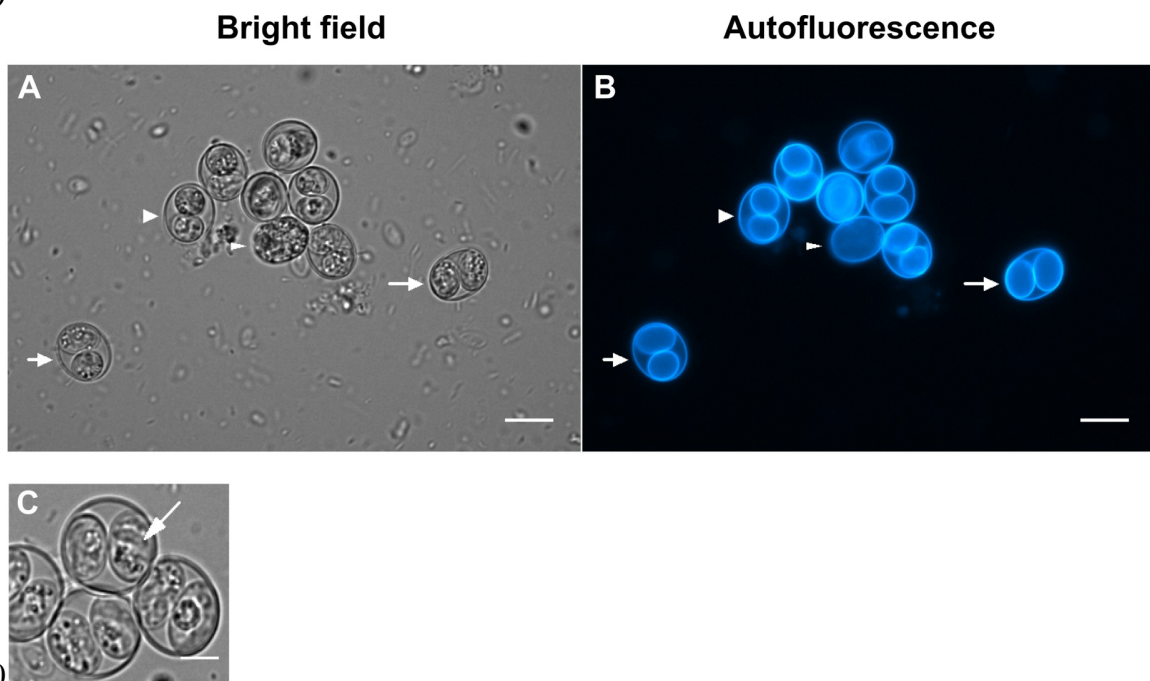
710

711SI Appendix Figures

712

713**Figure S1: *Toxoplasma gondii* oocyst subpopulations obtained after 5 days of sporu-**
 714**lation in water.** The suspension contained a mixture of different maturing stages of
 715oocysts. Observed unsporulated oocysts (NS, small arrowhead) were spherical and con-
 716tained a single granular mass (which corresponds to the zygote (6)), almost filling the
 717oocyst. Maturing oocysts containing two sporoblasts (SB, large arrowhead) were ovoid
 718and harbored two spherical sporoblasts, each filled with granular material. Fully sporu-
 719lated (SP) oocysts containing sporocysts (large arrow, and C) were ovoid in shape and
 720had two fully developed sporocysts containing four sporozoites each. Additionally,
 721oocysts at the SB-SP transition (small arrow), i.e. containing one sporoblast and one
 722sporocyst, were sometimes observed and were further recorded as SB oocysts (e.g. in
 723AFM experiments). Oocysts were observed under bright field (A) or UV excitation for
 724recording their autofluorescence pattern (B). Note the presence of fecal contaminants on
 725the bright field image. Scale bars = 10 μ m. (C) Fully sporulated *Toxoplasma gondii*
 726oocysts, under bright field, harboring two sporocysts containing four banana-shaped
 727sporozoite forms of the parasite. At least one sporozoite is very distinct in the picture (ar-
 728row). Scale bar = 5 μ m.

729

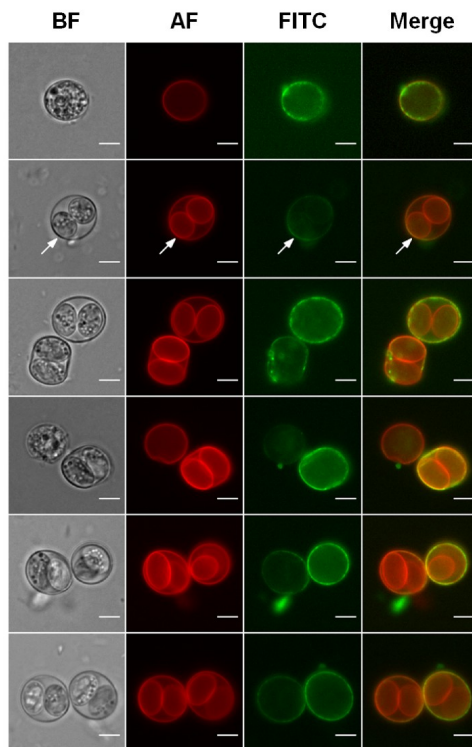


730

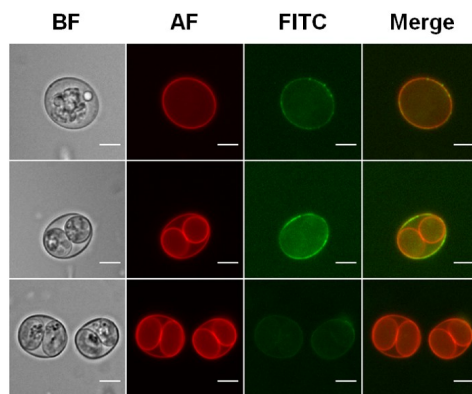
73
74

Figure S2: Fluorescence patterns of the wall of *T. gondii* oocysts exposed solely to H₂O (A), heated at 80°C (B), treated by bleach solution (C), or bleach- and then heat-treated (D) as described in the material and methods section. Oocysts were then allowed to react with 4B6 antibody specific to their inner wall (4, 5). BF, bright field; AF, autofluorescence under UV excitation (red channel); FITC corresponds to 4B6 fluorescence (green channel). Merge presents overlay between AF and FITC channel. Scale bars = 5 µm.

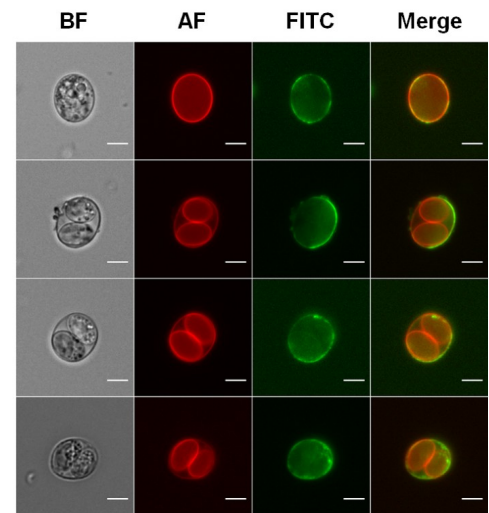
A



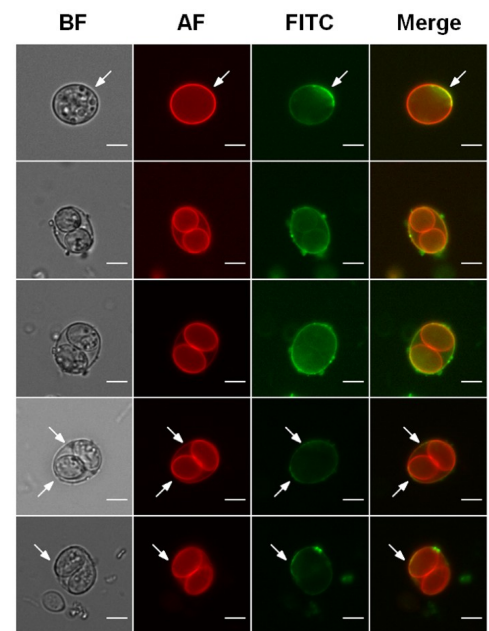
B



C



D



739
740
741
742
743
744
745
746
747
748
749

79
80

Figure S3: Fluorescein Infiltration Assay. (A) The permeability of the wall of *Toxoplasma gondii* oocysts exposed or not to bleach treatment was assessed by incubating oocysts with fluorescein isothiocyanate. BF, bright field; AF, autofluorescence under UV excitation (red); FITC, fluorescein isothiocyanate fluorescence (green). Scale bars = 5 μ m. (B) Percents of FITC permeable oocysts. No statistical difference was noted between control and bleach-treated oocysts at any maturing stage.

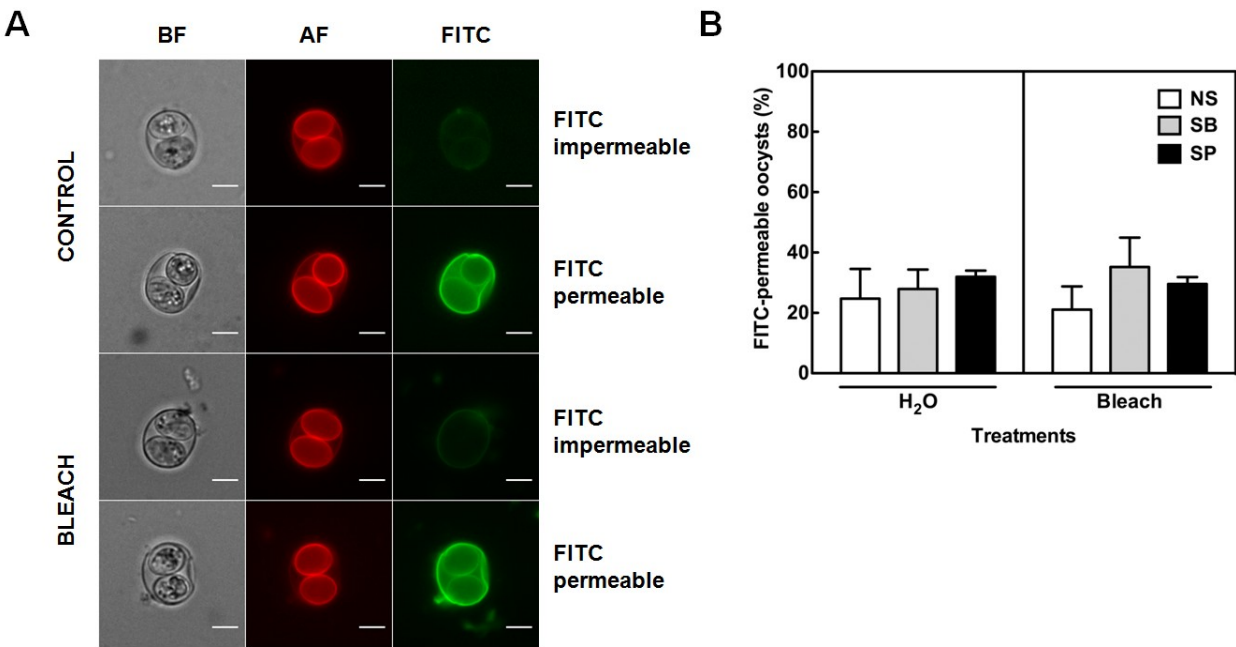
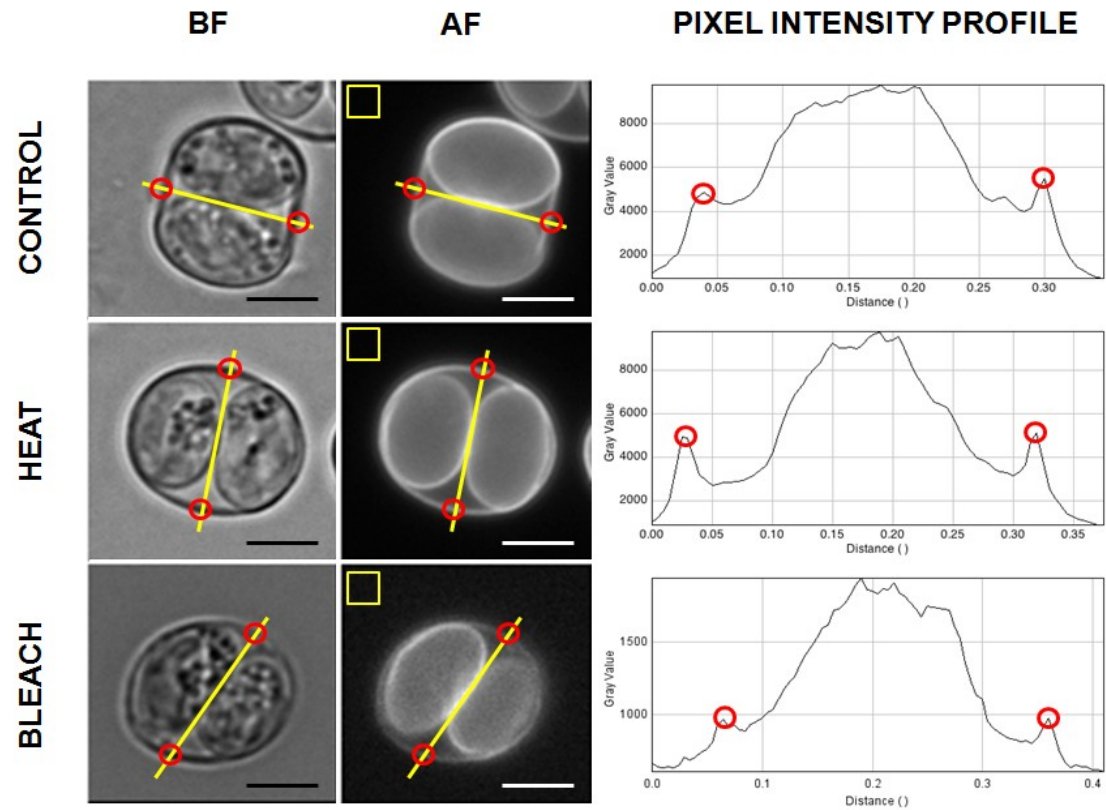


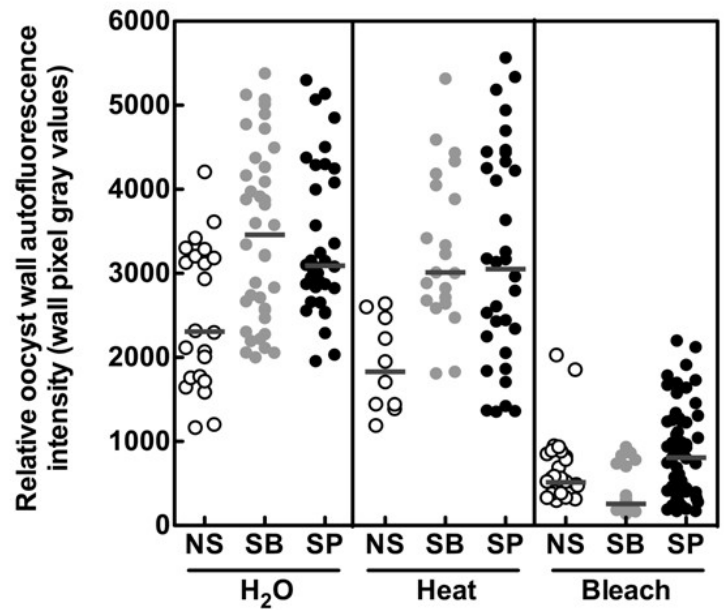
Figure S4: Quantification of the oocyst wall autofluorescence. (A) Control, heat- or bleach-treated oocysts were randomly examined microscopically under bright field (BF) and UV excitation (AF) (typically 10-35 oocysts per maturing stage and treatment condition). Their respective AF pattern was recorded as gray scale images. The relative oocyst wall AF intensity values were obtained by recording pixel gray values along a straight line (in yellow) arbitrarily set up across the width of each oocyst type. Values were plotted as a function of the pixel position along the selection line, and then normalized with regard to background gray value of each image (yellow square). Red circles indicate gray values of the oocyst wall that then were plotted in graph B. Scale bars= 5 μ m. (B) Distribution of the relative autofluorescence intensity of the oocyst wall. The line is the median of the distribution. Significant differences were observed when comparing NS vs. NS/bleach ($p < 0.001$), SB vs. SB/bleach ($p < 0.001$), SP vs. SP/bleach ($p < 0.001$), SB/heat vs. SB/bleach ($p < 0.001$), and SP/heat vs. SP/bleach ($p < 0.001$). No statistical difference was noted between control and heated oocysts at any maturing stage.

772
773

A



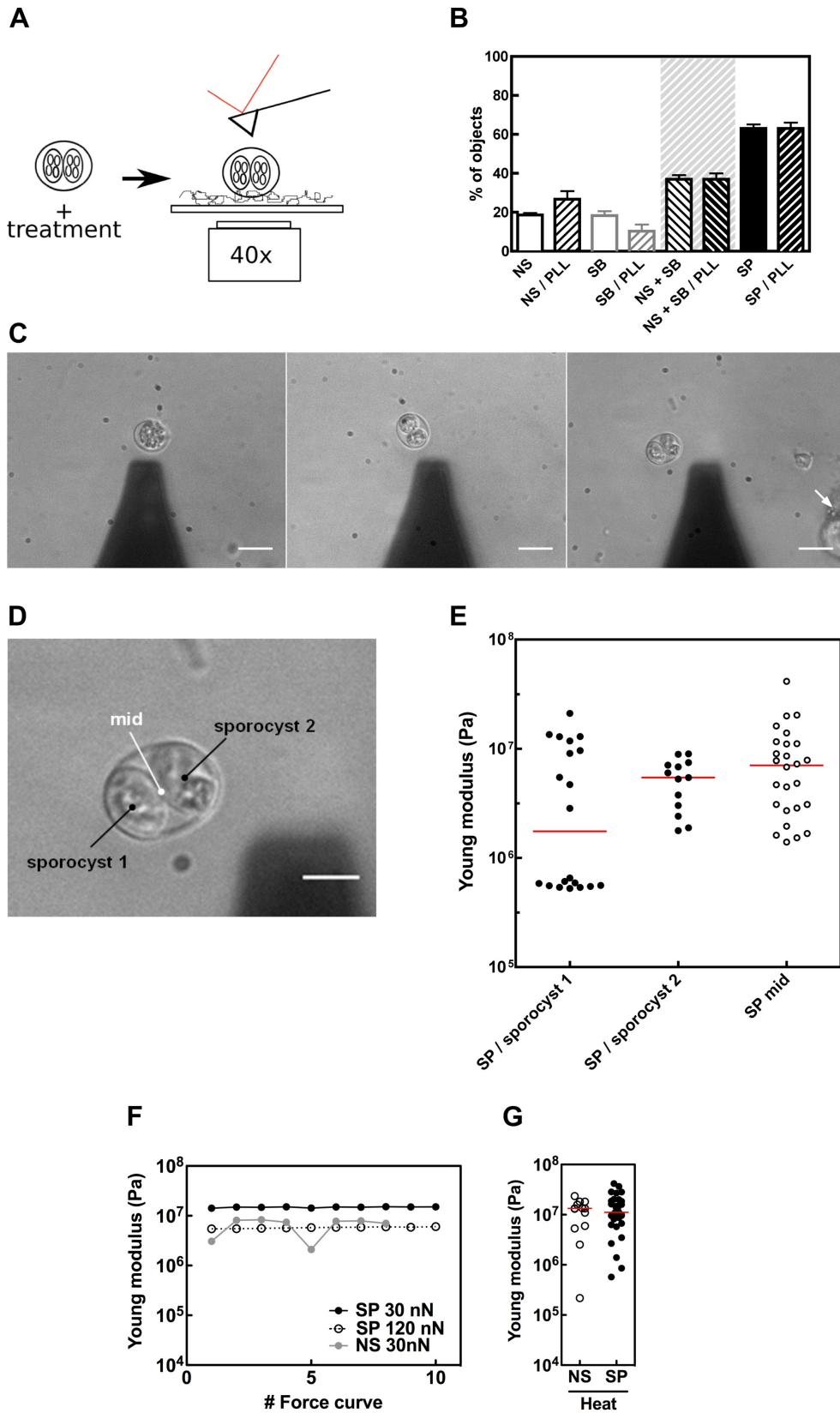
B



774

85
86

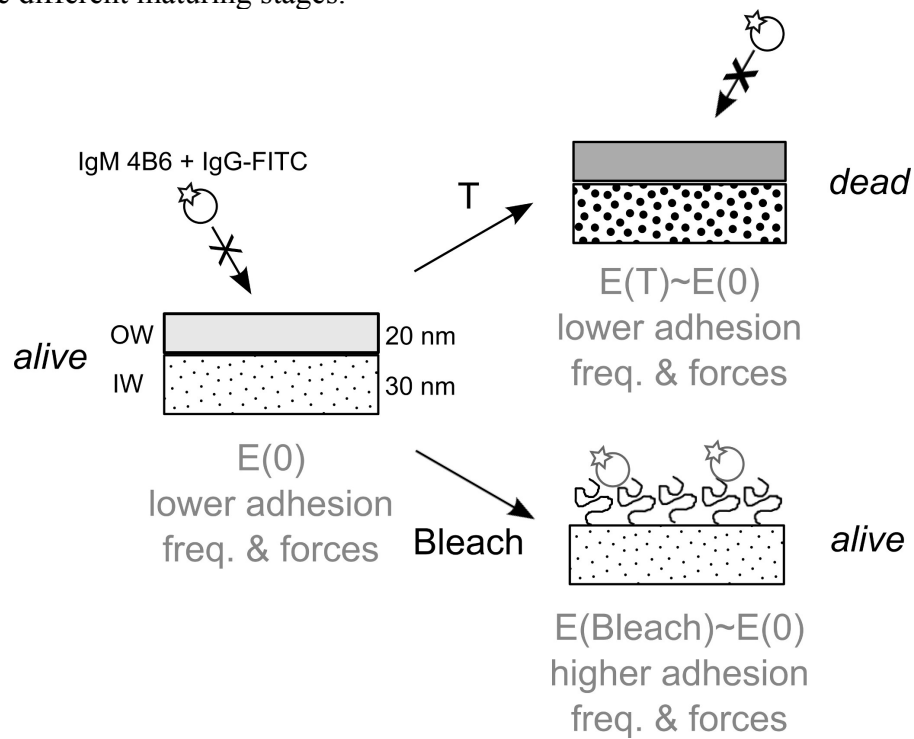
Figure S5: Attachment of the *Toxoplasma gondii* oocysts onto Poly-L-Lysine (PLL)-coated glass slides and positioning of the AFM tip on top of the adhered oocysts. (A) Schematics of the procedure. (B) Conservation of subpopulations of oocysts after transfer to PLL-coated surface compared to the subpopulations of the parasites from the original suspension, as a fraction of total observed objects. (C) NS (left), SB (middle) and SP (right) oocysts were imaged together with the AFM cantilever (i.e. the dark triangular-shape object on the pictures), showing that one can distinguish them easily while doing AFM. The presence of other fecal objects such as yeasts or larger objects (mainly fiber-like debris, arrow) invariably occurred because the oocysts we used for AFM experiments were extracted and stored in water with no additional chemicals to limit bacterial proliferation. Such non-target objects could be located near the oocysts, at the same focal plane, however they did not affect the overall AFM cantilever motions, except on rare occasions. In these latter cases, the corresponding force curves were not processed for further analyses. Scale bars = 10 μm . (D) Zoom on the same SP oocyst as in panel C. The calibrated AFM cantilever was positioned using micrometer screws on top of it (e.g. over the two sporocysts of SP oocysts and between them (mid position)). (E) Distribution of the Young modulus at each of the three positions of the AFM tip. The red line is the median of the distribution. No significant difference was observed (Kruskal-Wallis test, $p > 0.05$). No trace of the indentation can be seen in our optical magnification on the oocyst surface following indentation repetition. (F, G) Oocyst mechanics explored at higher contact forces. (F) Repeated measured values of Young modulus of 3 heated oocysts of two subtypes for heated oocyst samples, showing that for a given object no tendency can be observed when indenting with a maximal force 30 to 120 times the one used in our study. Note that the value of 10^4 Pa used as the lower limit of the scale corresponds to the values recorded for hard eukaryotic cells as found in literature. (G) Young modulus as a function of oocyst subtype. Each point is the value obtained for a single force curve. The red line is the median of the distribution. No significant difference is observed between the two cases and the measured medians are similar to the ones measured at 1 nN.



804
805

89
90

806 **Figure S6: Proposed structure of the bi-layered wall of the *Toxoplasma* oocyst in**
807 **terms of mechanics and adhesive properties.** Temperature and bleach treatments have
808 no effect on the oocyst wall mechanics but have opposite effect on wall adhesion and ac-
809 cessibility to inner wall by a specific antibody: bleached oocysts exhibit higher adhesion
810 frequency and forces than heated or control oocysts. Little differences are observed
811 among the different maturing stages.



812SI Appendix Tables

Table S1: Statistical analyses of the maximal indentation under a force of 1 nN as a function of oocyst subtype and treatment (see Fig. 3D). Data obtained with Prism 6 (GraphPad).

816

817Table Analyzed Indentation @ 1nN

818

819

820Kruskal-Wallis test

821

822P value 0,0145

823

824Exact or approximate P value? Approximate

825

826P value summary *

827

828Do the medians vary signif. ($P < 0.05$) Yes

829

830Number of groups 10

831

832Kruskal-Wallis statistic 20,60

833

834

835

836Data summary

837

838Number of treatments (columns) 10

839

840 Number of values (total) 115

841

842Number of families 1

843

844Number of comparisons per family 45

845

846Alpha 0,05

847

848

849

850Dunn's multiple comparisons test Mean rank diff, Significant? Adjusted P Value

851

852

853

854 NS vs. SB -2,622 No ns > 0,9999

855

856 NS vs. SP 1,861 No ns > 0,9999

857

858 NS vs. NS / T 33,46 No ns > 0,9999

859

860 NS vs. SP / T 30,20 No ns 0,8379

861

862 NS vs. NS / bleach 1,778 No ns > 0,9999

863

864 NS vs. SP / bleach 7,340 No ns > 0,9999

865

95

96

866	NS vs. NS / bleach / T	13,94	No	ns	> 0,9999
867					
868	NS vs. SB / bleach / T	-15,35	No	ns	> 0,9999
869					
870	NS vs. SP / bleach / T	5,369	No	ns	> 0,9999
871					
872	SB vs. SP	4,483	No	ns	> 0,9999
873					
874	SB vs. NS / T	36,08	No	ns	> 0,9999
875					
876	SB vs. SP / T	32,83	No	ns	> 0,9999
877					
878	SB vs. NS / bleach	4,400	No	ns	> 0,9999
879					
880	SB vs. SP / bleach	9,963	No	ns	> 0,9999
881					
882	SB vs. NS / bleach / T	16,57	No	ns	> 0,9999
883					
884	SB vs. SB / bleach / T	-12,73	No	ns	> 0,9999
885					
886	SB vs. SP / bleach / T	7,991	No	ns	> 0,9999
887					
888	SP vs. NS / T	31,60	No	ns	0,5983
889					
890	SP vs. SP / T	28,34	No	ns	0,2352
891					
892	SP vs. NS / bleach	-0,08333No	ns	> 0,9999	
893					
894	SP vs. SP / bleach	5,479	No	ns	> 0,9999
895					
896	SP vs. NS / bleach / T	12,08	No	ns	> 0,9999
897					
898	SP vs. SB / bleach / T	-17,21	No	ns	> 0,9999
899					
900	SP vs. SP / bleach / T	3,508	No	ns	> 0,9999
901					
902	NS / T vs. SP / T	-3,256	No	ns	> 0,9999
903					
904	NS / T vs. NS / bleach	-31,68	No	ns	> 0,9999
905					
906	NS / T vs. SP / bleach	-26,12	No	ns	> 0,9999
907					
908	NS / T vs. NS / bleach / T	-19,52	No	ns	> 0,9999
909					
910	NS / T vs. SB / bleach / T	-48,81	No	ns	0,5487
911					
912	NS / T vs. SP / bleach / T	-28,09	No	ns	> 0,9999
913					
914	SP / T vs. NS / bleach	-28,43	No	ns	> 0,9999
915					
916	SP / T vs. SP / bleach	-22,86	No	ns	> 0,9999
917					
918	SP / T vs. NS / bleach / T	-16,26	No	ns	> 0,9999
919					
920	SP / T vs. SB / bleach / T	-45,55	No	ns	0,4857
921					

922	SP / T vs. SP / bleach / T	-24,84	No	ns	0,4285
923					
924	NS / bleach vs. SP / bleach	5,563	No	ns	> 0,9999
925					
926	NS / bleach vs. NS / bleach / T	12,17	No	ns	> 0,9999
927					
928	NS / bleach vs. SB / bleach / T	-17,13	No	ns	> 0,9999
929					
930	NS / bleach vs. SP / bleach / T	3,591	No	ns	> 0,9999
931					
932	SP / bleach vs. NS / bleach / T	6,604	No	ns	> 0,9999
933					
934	SP / bleach vs. SB / bleach / T	-22,69	No	ns	> 0,9999
935					
936	SP / bleach vs. SP / bleach / T	-1,972	No	ns	> 0,9999
937					
938	NS / bleach / T vs. SB / bleach / T	-29,29	No	ns	> 0,9999
939					
940	NS / bleach / T vs. SP / bleach / T	-8,576	No	ns	> 0,9999
941					
942	SB / bleach / T vs. SP / bleach / T	20,72	No	ns	> 0,9999
943					

Table S2: Statistical analyses of the Young modulus as a function of oocyst subtype and treatment (see Fig. 3F). Data obtained with Prism 6 (GraphPad).

Table Analyzed Young Modulus

Kruskal-Wallis test

P value 0,0790

Exact or approximate P value? Approximate

P value summary ns

Do the medians vary signif. (P < 0.05) No

Number of groups 10

Kruskal-Wallis statistic 15,46

Data summary

Number of treatments (columns) 10

Number of values (total) 127

Number of families 1

Number of comparisons per family 45

Alpha 0,05

Dunn's multiple comparisons test	Mean rank diff,	Significant?	Adjusted P Value
SP / T vs. NS / T	2,998	No ns	> 0,9999
SP / T vs. SP / bleach	25,15	No ns	> 0,9999
SP / T vs. NS / bleach	28,15	No ns	> 0,9999
SP / T vs. SP	25,97	No ns	0,6446
SP / T vs. SB	30,15	No ns	> 0,9999
SP / T vs. NS	26,65	No ns	> 0,9999
SP / T vs. SP / bleach / T	29,03	No ns	0,1485

998					
999	SP / T vs. SB / bleach / T	29,75	No	ns	> 0,9999
1000					
1001	SP / T vs. NS / bleach / T	11,32	No	ns	> 0,9999
1002					
1003	NS / T vs. SP / bleach	22,15	No	ns	> 0,9999
1004					
1005	NS / T vs. NS / bleach	25,15	No	ns	> 0,9999
1006					
1007	NS / T vs. SP	22,97	No	ns	> 0,9999
1008					
1009	NS / T vs. SB	27,15	No	ns	> 0,9999
1010					
1011	NS / T vs. NS	23,65	No	ns	> 0,9999
1012					
1013	NS / T vs. SP / bleach / T	26,03	No	ns	> 0,9999
1014					
1015	NS / T vs. SB / bleach / T	26,75	No	ns	> 0,9999
1016					
1017	NS / T vs. NS / bleach / T	8,321	No	ns	> 0,9999
1018					
1019	SP / bleach vs. NS / bleach	3,000	No	ns	> 0,9999
1020					
1021	SP / bleach vs. SP	0,8158	No	ns	> 0,9999
1022					
1023	SP / bleach vs. SB	5,000	No	ns	> 0,9999
1024					
1025	SP / bleach vs. NS	1,500	No	ns	> 0,9999
1026					
1027	SP / bleach vs. SP / bleach / T	3,875	No	ns	> 0,9999
1028					
1029	SP / bleach vs. SB / bleach / T	4,600	No	ns	> 0,9999
1030					
1031	SP / bleach vs. NS / bleach / T	-13,83	No	ns	> 0,9999
1032					
1033	NS / bleach vs. SP	-2,184	No	ns	> 0,9999
1034					
1035	NS / bleach vs. SB	2,000	No	ns	> 0,9999
1036					
1037	NS / bleach vs. NS	-1,500	No	ns	> 0,9999
1038					
1039	NS / bleach vs. SP / bleach / T	0,8750	No	ns	> 0,9999
1040					
1041	NS / bleach vs. SB / bleach / T	1,600	No	ns	> 0,9999
1042					
1043	NS / bleach vs. NS / bleach / T	-16,83	No	ns	> 0,9999
1044					
1045	SP vs. SB	4,184	No	ns	> 0,9999
1046					
1047	SP vs. NS	0,6842	No	ns	> 0,9999
1048					
1049	SP vs. SP / bleach / T	3,059	No	ns	> 0,9999
1050					
1051	SP vs. SB / bleach / T	3,784	No	ns	> 0,9999
1052					
1053	SP vs. NS / bleach / T	-14,65	No	ns	> 0,9999

1054					
1055	SB vs. NS	-3,500	No	ns	> 0,9999
1056					
1057	SB vs. SP / bleach / T	-1,125	No	ns	> 0,9999
1058					
1059	SB vs. SB / bleach / T	-0,4000	No	ns	> 0,9999
1060					
1061	SB vs. NS / bleach / T	-18,83	No	ns	> 0,9999
1062					
1063	NS vs. SP / bleach / T	2,375	No	ns	> 0,9999
1064					
1065	NS vs. SB / bleach / T	3,100	No	ns	> 0,9999
1066					
1067	NS vs. NS / bleach / T	-15,33	No	ns	> 0,9999
1068					
1069	SP / bleach / T vs. SB / bleach / T	0,7250	No	ns	> 0,9999
1070					
1071	SP / bleach / T vs. NS / bleach / T	-17,71	No	ns	> 0,9999
1072					
1073	SB / bleach / T vs. NS / bleach / T	-18,43	No	ns	> 0,9999
1074					
1075					

Table S3: Statistical analyses of the distribution of adhesion forces as whisker plots for oocysts of different subtypes and treatments (see Fig. 4F). Data obtained with Prism 6 (GraphPad).

Table Analyzed	Adhesion Force			
Kruskal-Wallis test				
P value	< 0,0001			
Exact or approximate P value?	Approximate			
P value summary	****			
Do the medians vary signif. (P < 0.05)	Yes			
Number of groups	12			
Kruskal-Wallis statistic	216,2			
Data summary				
Number of treatments (columns)	12			
Number of values (total)	913			
Number of families	1			
Number of comparisons per family	66			
Alpha	0,05			
Dunn's multiple comparisons test	Mean rank diff,	Significant?	Adjusted P Value	
NS vs. SB	-15,39	No ns	> 0,9999	
NS vs. SP	-4,319	No ns	> 0,9999	
NS vs. NS / T	-42,15	No ns	> 0,9999	
NS vs. SB / T	-142,8	No ns	> 0,9999	
NS vs. SP / T	-60,13	No ns	> 0,9999	
NS vs. NS / bleach	-212,6	Yes **	0,0017	
NS vs. SB / bleach	-138,8	No ns	> 0,9999	
NS vs. SP / bleach	-332,5	Yes ****	< 0,0001	

1129				
1130	NS vs. NS / bleach / T	-308,4	Yes	**** < 0,0001
1131				
1132	NS vs. SB / bleach / T	-237,1	Yes	**** < 0,0001
1133				
1134	NS vs. SP / bleach / T	-278,8	Yes	**** < 0,0001
1135				
1136	SB vs. SP	11,07	No	ns > 0,9999
1137				
1138	SB vs. NS / T	-26,76	No	ns > 0,9999
1139				
1140	SB vs. SB / T	-127,4	No	ns > 0,9999
1141				
1142	SB vs. SP / T	-44,74	No	ns > 0,9999
1143				
1144	SB vs. NS / bleach	-197,2	No	ns 0,0629
1145				
1146	SB vs. SB / bleach	-123,4	No	ns > 0,9999
1147				
1148	SB vs. SP / bleach	-317,1	Yes	**** < 0,0001
1149				
1150	SB vs. NS / bleach / T	-293,1	Yes	**** < 0,0001
1151				
1152	SB vs. SB / bleach / T	-221,8	Yes	** 0,0087
1153				
1154	SB vs. SP / bleach / T	-263,4	Yes	**** < 0,0001
1155				
1156	SP vs. NS / T	-37,83	No	ns > 0,9999
1157				
1158	SP vs. SB / T	-138,4	No	ns > 0,9999
1159				
1160	SP vs. SP / T	-55,81	No	ns > 0,9999
1161				
1162	SP vs. NS / bleach	-208,2	Yes	*** 0,0003
1163				
1164	SP vs. SB / bleach	-134,5	No	ns > 0,9999
1165				
1166	SP vs. SP / bleach	-328,2	Yes	**** < 0,0001
1167				
1168	SP vs. NS / bleach / T	-304,1	Yes	**** < 0,0001
1169				
1170	SP vs. SB / bleach / T	-232,8	Yes	**** < 0,0001
1171				
1172	SP vs. SP / bleach / T	-274,4	Yes	**** < 0,0001
1173				
1174	NS / T vs. SB / T	-100,6	No	ns > 0,9999
1175				
1176	NS / T vs. SP / T	-17,98	No	ns > 0,9999
1177				
1178	NS / T vs. NS / bleach	-170,4	No	ns 0,0985
1179				
1180	NS / T vs. SB / bleach	-96,67	No	ns > 0,9999
1181				
1182	NS / T vs. SP / bleach	-290,4	Yes	**** < 0,0001
1183				
1184	NS / T vs. NS / bleach / T	-266,3	Yes	**** < 0,0001

1185					
1186	NS / T vs. SB / bleach / T	-195,0	Yes	*	0,0109
1187					
1188	NS / T vs. SP / bleach / T	-236,6	Yes	****	< 0,0001
1189					
1190	SB / T vs. SP / T	82,64	No	ns	> 0,9999
1191					
1192	SB / T vs. NS / bleach	-69,79	No	ns	> 0,9999
1193					
1194	SB / T vs. SB / bleach	3,946	No	ns	> 0,9999
1195					
1196	SB / T vs. SP / bleach	-189,7	No	ns	> 0,9999
1197					
1198	SB / T vs. NS / bleach / T	-165,7	No	ns	> 0,9999
1199					
1200	SB / T vs. SB / bleach / T	-94,38	No	ns	> 0,9999
1201					
1202	SB / T vs. SP / bleach / T	-136,0	No	ns	> 0,9999
1203					
1204	SP / T vs. NS / bleach	-152,4	Yes	*	0,0298
1205					
1206	SP / T vs. SB / bleach	-78,69	No	ns	> 0,9999
1207					
1208	SP / T vs. SP / bleach	-272,4	Yes	****	< 0,0001
1209					
1210	SP / T vs. NS / bleach / T	-248,3	Yes	****	< 0,0001
1211					
1212	SP / T vs. SB / bleach / T	-177,0	Yes	**	0,0011
1213					
1214	SP / T vs. SP / bleach / T	-218,6	Yes	****	< 0,0001
1215					
1216	NS / bleach vs. SB / bleach	73,73	No	ns	> 0,9999
1217					
1218	NS / bleach vs. SP / bleach	-120,0	No	ns	0,7992
1219					
1220	NS / bleach vs. NS / bleach / T	-95,88	No	ns	> 0,9999
1221					
1222	NS / bleach vs. SB / bleach / T	-24,59	No	ns	> 0,9999
1223					
1224	NS / bleach vs. SP / bleach / T	-66,22	No	ns	> 0,9999
1225					
1226	SB / bleach vs. SP / bleach	-193,7	No	ns	> 0,9999
1227					
1228	SB / bleach vs. NS / bleach / T	-169,6	No	ns	> 0,9999
1229					
1230	SB / bleach vs. SB / bleach / T	-98,33	No	ns	> 0,9999
1231					
1232	SB / bleach vs. SP / bleach / T	-139,9	No	ns	> 0,9999
1233					
1234	SP / bleach vs. NS / bleach / T	24,08	No	ns	> 0,9999
1235					
1236	SP / bleach vs. SB / bleach / T	95,36	No	ns	> 0,9999
1237					
1238	SP / bleach vs. SP / bleach / T	53,74	No	ns	> 0,9999
1239					
1240	NS / bleach / T vs. SB / bleach / T	71,29	No	ns	> 0,9999

1241				
1242	NS / bleach / T vs. SP / bleach / T 29,67	No	ns	> 0,9999
1243				
1244	SB / bleach / T vs. SP / bleach / T -41,62	No	ns	> 0,9999

Table S4: Summary of median values of indentation, *E* moduli, and adhesion force of *Toxoplasma* oocysts at different maturing stages following different surface treatments. n = conserved data points.

	H ₂ O			Heat			Bleach			Bleach→heat		
	NS	SB	SP	NS	SB	SP	NS	SB	SP	NS	SB	SP
Indentation (nm)	22,5	22,6	20,5	11,4	8,60	12,4	17,0	15,0	18,5	16,8	23,9	17,1
n (oocysts)	9	5	18	11	1	27	5	1	8	6	4	22
<i>E</i> modulus (MPa)	5.3	2.8	4.2	11.1	22.2	11.1	7.9	14.0	5.7	8.8	5.0	6.0
n (oocysts)	9	5	19	13	1	33	5	1	8	6	5	24
Adhesion force (pN)	85,0	79,5	75,5	86,0	100,0	94,5	184,5	134,5	246,0	244,5	197,0	234,0
n (force curves)	67	34	124	51	7	186	46	8	90	60	53	187

1247

1248SI Appendix Reference list

1249

125060. Dubey JP et al. (2011) Isolation of viable *Toxoplasma gondii* from feral guinea fowl (*Numida*
1251 *meleagris*) and domestic rabbits (*Oryctolagus cuniculus*) from Brazil. *J Parasitol* 97:842–
1252 845.

125361. Fritz HM et al. (2012) Transcriptomic analysis of *Toxoplasma* development reveals many
1254 novel functions and structures specific to sporozoites and oocysts. *PLoS ONE* 7:e29998.

125562. Dubey JP, Miller NL, Frenkel JK (1970) The *Toxoplasma gondii* oocyst from cat feces. *J Exp*
1256 *Med* 132:636–662.

125763. Dumètre A, Dardé M-L (2007) Detection of *Toxoplasma gondii* in water by an
1258 immunomagnetic separation method targeting the sporocysts. *Parasitol Res* 101:989–996.

125964. Dumètre A, Dardé M-L (2005) Immunomagnetic separation of *Toxoplasma gondii* oocysts
1260 using a monoclonal antibody directed against the oocyst wall. *J Microbiol Methods* 61:209–
1261 217.

126265. Ferguson DJ, Birch-Andersen A, Siim JC, Hutchison WM (1979) Ultrastructural studies on
1263 the sporulation of oocysts of *Toxoplasma gondii*. I. Development of the zygote and formation
1264 of the sporoblasts. *Acta Pathol Microbiol Scand B* 87B:171–181.

1265

1266

1267

1268

1269

1271

1272

1273

117

118